Chapter 2
Elementary Electromagnetic Phenomena

All the effects discussed in this text rely on the presence of electric, magnetic or electro-magnetic fields in the system. It is therefore natural to discuss first the governing equations and some basic electromagnetic phenomena. With this regard, "elementary" in the title of this chapter refers to subjects related to beam-wave interaction and not necessarily to undergraduate-level topics, though we discuss a few elementary concepts in the first two subsections.

2.1 Maxwell's Equations

At the foundations for the analysis of all electro-magnetic phenomena are Maxwell's equations that relate the electric (**E**) and magnetic (**H**) field, the electric (**D**) and magnetic (**B**) inductions with the current (**J**) and charge (ρ) densities:

$$\nabla \times \mathbf{E}(\mathbf{r},t) + \frac{\partial}{\partial t}\mathbf{B}(\mathbf{r},t) = 0, \tag{2.1.1}$$

$$\nabla \times \mathbf{H}(\mathbf{r},t) - \frac{\partial}{\partial t}\mathbf{D}(\mathbf{r},t) = \mathbf{J}(\mathbf{r},t), \tag{2.1.2}$$

$$\nabla \cdot \mathbf{D}(\mathbf{r},t) = \rho(\mathbf{r},t), \tag{2.1.3}$$

$$\nabla \cdot \mathbf{B}(\mathbf{r},t) = 0. \tag{2.1.4}$$

This set of equations determines the electromagnetic field at any point in space and in time provided that the source terms (ρ and **J**), are known. In addition, the initial and boundary conditions have to be determined together with the constitutive relations of the medium, i.e., the relation between the inductions (**B** and **D**) and the field components (**H** and **E**).

L. Schächter, *Beam-Wave Interaction in Periodic and Quasi-Periodic Structures*, Particle Acceleration and Detection, DOI 10.1007/978-3-642-19848-9_2,

2.1.1 Constitutive Relations

Matter reacts to the presence of an electromagnetic field and the constitutive relations characterize this reaction. In general, these relations are non-linear and they couple all the components of the electromagnetic field. In many of the cases of interest, the constitutive relations are linear and scalar

$$\mathbf{B}(\mathbf{r},t) = \mu_0\mu_\mathrm{r}\mathbf{H}(\mathbf{r},t), \tag{2.1.5}$$

$$\mathbf{D}(\mathbf{r},t) = \varepsilon_0\varepsilon_\mathrm{r}\mathbf{E}(\mathbf{r},t), \tag{2.1.6}$$

and in case of a metal Ohm law's reads

$$\mathbf{J}(\mathbf{r},t) = \sigma\mathbf{E}(\mathbf{r},t); \tag{2.1.7}$$

here $\varepsilon_0 = 8.85 \times 10^{-12}$ farad/m and $\mu_0 = 4\pi \times 10^{-7}$ henry/m are the vacuum permittivity and permeability respectively. The *relative* dielectric coefficient ε_r and its permeability counterpart μ_r characterize the material. In vacuum, $\varepsilon_\mathrm{r} \equiv 1$, $\mu_\mathrm{r} \equiv 1$ and $\sigma = 0$, i.e.,

$$\nabla \times \mathbf{E}(\mathbf{r},t) + \frac{\partial}{\partial t}\mu_0\mathbf{H}(\mathbf{r},t) = 0, \tag{2.1.8}$$

$$\nabla \times \mathbf{H}(\mathbf{r},t) - \frac{\partial}{\partial t}\varepsilon_0\mathbf{E}(\mathbf{r},t) = \mathbf{J}(\mathbf{r},t), \tag{2.1.9}$$

$$\nabla \cdot \varepsilon_0\mathbf{E}(\mathbf{r},t) = \rho(\mathbf{r},t), \tag{2.1.10}$$

$$\nabla \cdot \mu_0\mathbf{H}(\mathbf{r},t) = 0. \tag{2.1.11}$$

Assuming that we know the source terms (ρ and $\mathbf{J}$) it is sufficient to use the first two equations (2.1.7)–(2.1.8) in conjunction with the charge conservation,

$$\nabla \cdot \mathbf{J}(\mathbf{r},t) + \frac{\partial}{\partial t}\rho(\mathbf{r},t) = 0, \tag{2.1.12}$$

in order to solve the electromagnetic field. This statement can be examined by applying $\nabla\cdot$ on both (2.1.7) and (2.1.8). Since any vector function $\mathbf{V}$ satisfies $\nabla \cdot (\nabla \times \mathbf{V}) \equiv 0$, one obtains (2.1.10) from (2.1.7) and (2.1.9) from (2.1.8).

2.1.2 Boundary Conditions

At sharp discontinuities the differential operators are not defined therefore an integral approach has to be adopted. Alternatively, Maxwell's equations can be

solved in each region separately, away of the discontinuity, and the question that needs to be addressed is the relation between the various field components from both sides of a discontinuity. Consider two regions (subscripts 1 and 2) separated by a surface which is locally characterized by its local normal $\mathbf{n}$. The boundary condition associated with (2.1.1) is deduced from its integral form as

$$\mathbf{n} \times (\mathbf{E}_1 - \mathbf{E}_2) = 0. \tag{2.1.13}$$

Similarly, from the integral form of (2.1.1) we conclude that

$$\mathbf{n} \times (\mathbf{H}_1 - \mathbf{H}_2) = \mathbf{J}_s, \tag{2.1.14}$$

from (2.1.2)

$$\mathbf{n} \cdot (\mathbf{D}_1 - \mathbf{D}_2) = \rho_s, \tag{2.1.15}$$

and finally, from the integral form of (2.1.3) we can deduce that

$$\mathbf{n} \cdot (\mathbf{B}_1 - \mathbf{B}_2) = 0. \tag{2.1.16}$$

Here $\mathbf{J}_s$ is the surface current density and ρ_s is the surface charge density.

Equation (2.1.12) indicates that the tangential component of the electric field, at any time, has to be continuous at the transition between two discontinuities. In a similar way, the tangential component of the magnetic field can be discontinuous only if there is a *surface current density* ($\mathbf{J}_s$) – see (2.1.13). The other two expressions indicate that any discontinuity in the normal component of the electric induction is due to surface charge density (ρ_s) and the normal component of the magnetic induction is always continuous.

Comment 2.1. As in the case of Maxwell's equations, it is sufficient to use the first two sets of boundary conditions since the latter two are then automatically satisfied.

Comment 2.2. One outcome of the boundary conditions as formulated above is that at the surface of an ideal metal ($\sigma \to \infty$) the tangential electric field vanishes. This is because the electric field is zero in the metal and the tangential electric field has to be continuous.

2.1.3 Poynting's Theorem

The energy conservation associated with the electromagnetic field can be deduced from Maxwell's equations by multiplying (scalarly) (2.1.1) by $\mathbf{H}$, (2.1.1) by $\mathbf{E}$ and subtracting the latter from the former. In a linear medium, the result reads

$$\nabla \cdot \mathbf{S} + \frac{\partial}{\partial t}\left[\frac{1}{2}\varepsilon_0\varepsilon_r \mathbf{E}\cdot\mathbf{E} + \frac{1}{2}\mu_0\mu_r \mathbf{H}\cdot\mathbf{H}\right] = -\mathbf{J}\cdot\mathbf{E}, \tag{2.1.17}$$

where

$$\mathbf{S}(\mathbf{r},t) \equiv \mathbf{E}(\mathbf{r},t)\times\mathbf{H}(\mathbf{r},t) \tag{2.1.18}$$

is the instantaneous *Poynting vector* which represents the energy flux (power per unit surface) in the vector direction. The second term,

$$\mathrm{w}(\mathbf{r},t) \equiv \frac{1}{2}\varepsilon_0\varepsilon_r \mathbf{E}(\mathbf{r},t)\cdot\mathbf{E}(\mathbf{r},t) + \frac{1}{2}\mu_0\mu_r \mathbf{H}(\mathbf{r},t)\cdot\mathbf{H}(\mathbf{r},t), \tag{2.1.19}$$

represents the instantaneous *energy density* stored in the electric and magnetic field respectively. And the right-hand side term in (2.1.16) represents the coupling between the electromagnetic field and the sources (or sinks) in the system.

Gauss's theorem can be used to formulate Poynting's theorem in its *integral form*. We integrate over a volume V whose boundary is denoted by **a**; the result is

$$\frac{\mathrm{d}}{\mathrm{d}t}W(t) = -\oiint \mathrm{d}\mathbf{a}\cdot S - \int_v \mathrm{d}V\mathbf{J}\cdot\mathbf{E}, \tag{2.1.20}$$

where for a linear medium

$$W(t) \equiv \int_V \mathrm{d}V\left[\frac{1}{2}\varepsilon_0\varepsilon_r \mathbf{E}\cdot\mathbf{E} + \frac{1}{2}\mu_0\mu_r \mathbf{H}\cdot\mathbf{H}\right], \tag{2.1.21}$$

is the total energy stored in the volume V. Explicitly (2.1.19) reveals that the change in the energy stored in the volume is either due to energy flux flowing *through* the surrounding envelope or due to sources in the volume (or both).

One important aspect to emphasize at this stage is that the electromagnetic power is carried by the field and not by the metallic boundaries; the latter only guide the energy flow. This is an important observation since subsequently, we discuss the propagation of electromagnetic waves of hundreds of megawatts and all this power propagates in vacuum. To illustrate the process let us consider an elementary electric circuit consisting of a battery, two parallel lossless wires, and a resistor at the end as illustrated in Fig. 2.1.

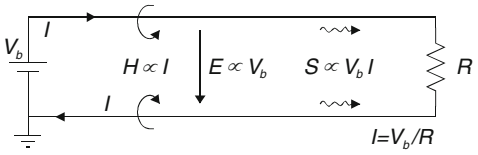

Fig. 2.1 Energy flow in a simple circuit. The power flows in the air and is guided by the wires

Firstly, we examine the Poynting vector term of (2.1.19): the voltage V_b is determined by the battery whereas the current is determined by the resistor (R) namely, $I = V_b/R$. Since the distance between the two wires is d, the typical electric field between the two wires is V_b/d moreover, the azimuthal magnetic field generated by one wire at the location of the other is proportional to the current I. Consequently, the Poynting vector is parallel to the wires and it is proportional to the product of the two field components $S \propto IV_b$. The power which propagates from the battery towards the resistor is proportional to Poynting vector thus as expected, the power is proportional to IV_b or V_b^2/R. Since there are no time variations the energy term in Poynting theorem vanishes whereas the second term in the right-hand side of (2.1.19) can be readily calculated to show that the power dissipated in the resistor is V_b^2/R. For further discussion see Chap. 11 in the text book of Haus and Melcher (1989).

2.1.4 Steady-State Regime

In many cases of interest all the components of the electromagnetic field oscillates at a single angular frequency (ω) thus all components have the following functional form

$$F(\mathbf{r},t) = f(\mathbf{r})\cos[\omega t + \psi(\mathbf{r})]. \tag{2.1.22}$$

It is convenient to omit the time dependence and represent the function $F(\mathbf{r},t)$ using a complex notation, namely we introduce the imaginary number $j \equiv \sqrt{-1}$ and utilize the fact that $\exp(j\xi) \equiv \cos(\xi) + j\sin(\xi)$ the function F

$$F(\mathbf{r},t) = \frac{1}{2}\{f(\mathbf{r})\exp[j\psi(\mathbf{r})]\exp(j\omega t) + f(\mathbf{r})\exp[-j\psi(\mathbf{r})]\exp(-j\omega t)\}. \tag{2.1.23}$$

With this notation, it is convenient to define

$$\bar{F}(\mathbf{r},\omega) \equiv f(\mathbf{r})e^{j\psi(\mathbf{r})}, \tag{2.1.24}$$

which permits us to use this function instead of $F(\mathbf{r},t)$ and consequently,

$$F(\mathbf{r},t) = \mathrm{Re}\left[\bar{F}(\mathbf{r},\omega)e^{j\omega t}\right]; \tag{2.1.25}$$

$\bar{F}(\mathbf{r},\omega)$ is called the *phasor* associated with the function $F(\mathbf{r},t)$. To illustrate the use of this notation, Maxwell's equations read

$$\nabla \times \overline{\mathbf{E}} + j\omega\overline{\mathbf{B}} = 0, \tag{2.1.26}$$

$$\nabla \times \overline{\mathbf{H}} - j\omega\overline{\mathbf{D}} = \overline{\mathbf{J}}, \tag{2.1.27}$$

$$\nabla \cdot \overline{\mathbf{D}} = \overline{\rho}, \tag{2.1.28}$$

$$\nabla \cdot \overline{\mathbf{B}} = 0. \tag{2.1.29}$$

The main advantage of this notation is now evident since the differential operator $\partial/\partial t$ was replaced by a simple algebraic operator $j\omega$.

2.1.5 Complex Poynting's Theorem

The phasor notation, as introduced above, cannot be directly applied to Poynting's theorem since all quantities are quadratic in the electromagnetic field. In principle, we have two options: (1) transform the field components to the time domain and then substitute in Poynting's theorem as defined in (2.1.16) – abandoning in the process the phasor notation. (2) Limit the information to the *average energy* and *average power* – but preserving the phasor notation. Since in the former case there is no real advantage to the new notation, we next pursue the latter option.

When we consider the product of two oscillating quantities, we have

$$\begin{aligned} &A_1 \cos(\omega t + \psi_1) A_2 \cos(\omega t + \psi_2) \\ &\quad = \frac{1}{4}\left[\bar{A}_1 \exp(j\omega t) + \bar{A}_1^* \exp(-j\omega t)\right]\left[\bar{A}_2 \exp(j\omega t) + \bar{A}_2^* \exp(-j\omega t)\right] \end{aligned} \tag{2.1.30}$$

the *average* of the product of these two oscillating functions corresponds to the non-oscillating term in the expression above i.e.,

$$\frac{1}{4}\left[\bar{A}_1\bar{A}_2^* + \bar{A}_1^*\bar{A}_2\right] = \frac{1}{2}A_1A_2\cos(\psi_1 - \psi_2). \tag{2.1.31}$$

We use this fact in order to formulate the *complex Poynting's theorem*. First (2.1.25) is multiplied scalarly by the complex conjugate of the magnetic field phasor ($\overline{\mathbf{H}}^*$). From the product we subtract the complex conjugate of (2.1.26) multiplied by the electric field; the result reads

$$\nabla \cdot \overline{\mathbf{S}} + 2j\omega[\overline{w}_M - \overline{w}_E] = -\frac{1}{2}\overline{\mathbf{E}} \cdot \overline{\mathbf{J}}^*, \tag{2.1.32}$$

wherein $\overline{\mathbf{S}} = \overline{\mathbf{E}} \times \overline{\mathbf{H}}^*/2$ is the *complex Poynting vector*, $\overline{w}_M = \mu_0\mu_r\overline{\mathbf{H}} \cdot \overline{\mathbf{H}}^*/4$ is the average (in time) magnetic energy density and $\overline{w}_E = \varepsilon_0\varepsilon_r\overline{\mathbf{E}} \cdot \overline{\mathbf{E}}^*/4$ is the electric counterpart.

Energy conversion is associated with the *real* part of the Poynting vector whereas the *imaginary* component is associated with electro-magnetic energy stored in the system. Throughout the text we omit the bar from the phasor quantities, except if ambiguities may occur.

2.1.6 Potentials

It is convenient, instead of solving a couple of first order differential equations, to solve a single second-order differential equation. For this purpose we benefit from the fact that the divergence of the magnetic induction is zero ($\nabla \cdot \mathbf{B} = 0$) and introduce the magnetic vector potential $\mathbf{A}$ which determines the magnetic induction through

$$\mathbf{B} = \nabla \times \mathbf{A} \tag{2.1.33}$$

By virtue of this definition, the equation $\nabla \cdot \mathbf{B} = 0$ becomes an identity. Substituting this definition in Faraday's law (2.1.25) we obtain

$$\nabla \times (\mathbf{E} + j\omega \mathbf{A}) = 0. \tag{2.1.34}$$

Further using the fact that $\nabla \times (\nabla \Phi) \equiv 0$ we conclude that

$$\mathbf{E} = -j\omega \mathbf{A} - \nabla \Phi, \tag{2.1.35}$$

wherein Φ is the *scalar electric potential*. Both potentials satisfy, in a Cartesian coordinate system and in a linear medium ($\mu_r = 1$ and $\varepsilon_r > 1$), the non-homogeneous wave equation:

$$\left[\nabla^2 + \varepsilon_r \frac{\omega^2}{c^2}\right] \mathbf{A} = -\mu_0 \mathbf{J}, \tag{2.1.36}$$

and

$$\left[\nabla^2 + \varepsilon_r \frac{\omega^2}{c^2}\right] \Phi = -\frac{1}{\varepsilon_0 \varepsilon_r} \rho, \tag{2.1.37}$$

provided that the divergence of the vector function $\mathbf{A}$ is chosen to be

$$\nabla \cdot \mathbf{A} + j\omega \frac{\varepsilon_r}{c^2} \Phi = 0. \tag{2.1.38}$$

This is the so-called *Lorentz gauge*; $c \equiv 1/\sqrt{\mu_0 \varepsilon_0}$ is the phase velocity of a plane electromagnetic wave in vacuum.

2.1.7 Edge Effect

In addition to the boundary conditions discussed above in the context of sharp discontinuity, we need to consider the field and the energy near an edge. It is demonstrated in what follows that while near an edge, the electric field diverges, the energy stored is finite.

With this purpose in mind, consider a simple configuration where the radius of curvature of a realistic edge is much smaller than the characteristic wavelength of the electromagnetic field in its vicinity ($\lambda \gg R$). Based on this assumption, the electric field in the vicinity of an ideal edge ($R = 0$) as the one schematically illustrated in Fig. 2.2, is a solution of the Laplace's equation and further assuming that the system is infinite in the z-direction, then

$$\left[\frac{1}{r}\frac{\partial}{\partial r}r\frac{\partial}{\partial r}+\frac{1}{r^2}\frac{\partial^2}{\partial \phi^2}\right]\Phi = 0 \tag{2.1.39}$$

is the equation to be solved subject to the zero potential condition on the metallic walls

$$\Phi\left(r, \phi = \frac{\alpha}{2}\right) = 0 \quad \text{and} \quad \Phi\left(r, \phi = 2\pi - \frac{\alpha}{2}\right) = 0. \tag{2.1.40}$$

Its solution has the form $\Phi \sim Ae^{jv\phi}r^v + Be^{-jv\phi}r^v$, thus imposing the boundary conditions namely, $\Phi(r, \phi = \alpha/2) = 0$ and $\Phi(r, \phi = 2\pi - \alpha/2) = 0$ we conclude that a non-trivial solution is possible if $\sin[v(2\pi - \alpha)] = 0$, implying that the radius of curvature of the field (v) is given by

$$v = \frac{\pi}{2\pi - \alpha}n \qquad n = 1, 2, 3 \ldots \tag{2.1.41}$$

and consequently,

$$\Phi\left(r, \frac{\alpha}{2} \leq \phi \leq 2\pi - \frac{\alpha}{2}\right) = \sum_{n=1}^{\infty} A_n \sin\left[\frac{\pi n}{2\pi - \alpha}\left(\phi - \frac{\alpha}{2}\right)\right] r^{\frac{\pi n}{2\pi - \alpha}}. \tag{2.1.42}$$

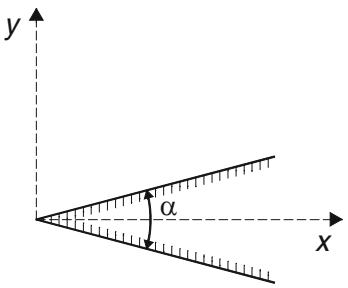

Fig. 2.2 In the vicinity of an ideal edge the curvature of the electric field is determined by its angle α

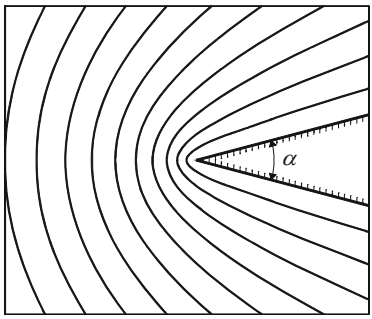

Fig. 2.3 Contours of constant potential $(n = 1)$ in the vicinity of an ideal edge

In order to demonstrate the previous statement, let us consider the first harmonic $(n = 1)$ illustrated in Fig. 2.3 for $\alpha = \pi/6$. The corresponding field components are

$$\begin{aligned} E_r &= -\frac{\partial \Phi_1}{\partial r} = -\frac{\pi}{2\pi - \alpha} A_1 \sin\left[\frac{\pi}{2\pi - \alpha}\left(\phi - \frac{\alpha}{2}\right)\right] r^{\frac{\pi}{2\pi-\alpha}-1} \\ E_\phi &= -\frac{1}{r}\frac{\partial \Phi_1}{\partial \phi} = -\frac{\pi}{2\pi - \alpha} A_1 \cos\left[\frac{\pi}{2\pi - \alpha}\left(\phi - \frac{\alpha}{2}\right)\right] r^{\frac{\pi}{2\pi-\alpha}-1} \end{aligned} \tag{2.1.43}$$

revealing that at the limit $r \to 0$, if $\alpha < \pi$, then the electric field *diverges*. Nevertheless, the energy, stored in a volume of radius R and length Δ_z, is *finite* as can be deduced from the explicit expression for the stored energy

$$W_E = \Delta_z \int_{\alpha/2}^{2\pi-\alpha/2} d\phi \int_0^R dr r \left[\frac{1}{2}\varepsilon_0 E_r^2 + \frac{1}{2}\varepsilon_0 E_\phi^2\right] \propto A_1^2 R \frac{2\pi}{2\pi - \alpha}. \tag{2.1.44}$$

Comment 2.3. A similar approach may be followed to investigate the field distribution in the vicinity of a *dielectric* edge. In this case the curvature of the field (v) is determined by both the angle of the edge (α) as well as the dielectric coefficient (ε_r) and it is a solution of

$$\varepsilon_r \tan\left(v\frac{\alpha}{2}\right) + \tan\left[v\left(\pi - \frac{\alpha}{2}\right)\right] = 0. \tag{2.1.45}$$

2.1.8 Reciprocity Theorem

The Lorentz reciprocity theorem is a useful theorem for solution of electromagnetic problems, since it may be used to deduce a number of fundamental properties of practical devices. It provides the basis for demonstrating the reciprocal properties of electronic microwave circuits and for showing that the receiving and transmitting characteristics of antennas are the same. To derive the theorem, consider a volume

V bounded by a closed surface A. Let a current source $\vec{J}_1$ in V produce a field $\vec{E}_1, \vec{H}_1$ while a second source $\vec{J}_2$ produces a field $\vec{E}_2, \vec{H}_2$. Expanding the relation $\nabla \cdot (\vec{E}_1 \times \vec{H}_2 - \vec{E}_2 \times \vec{H}_1)$ and using Maxwell's equation it can be shown that

$$\begin{aligned} \nabla \cdot (\vec{E}_1 \times \vec{H}_2 - \vec{E}_2 \times \vec{H}_1) &= (\nabla \times \vec{E}_1) \cdot \vec{H}_2 - (\nabla \times \vec{H}_2) \cdot \vec{E}_1 \\ &\quad - (\nabla \times \vec{E}_2) \cdot \vec{H}_1 + (\nabla \times \vec{H}_1) \cdot \vec{E}_2 \\ &= -\vec{J}_2 \cdot \vec{E}_1 + \vec{J}_1 \cdot \vec{E}_2. \end{aligned} \tag{2.1.46}$$

Integrating both sides over the volume V and using Gauss' theorem

$$\begin{aligned} \int_V \nabla \cdot (\vec{E}_1 \times \vec{H}_2 - \vec{E}_2 \times \vec{H}_1) dV &= \oiint_A (\vec{E}_1 \times \vec{H}_2 - \vec{E}_2 \times \vec{H}_1) \cdot \vec{n} dA \\ &= \int_V (\vec{E}_2 \cdot \vec{J}_1 - \vec{E}_1 \cdot \vec{J}_2) dV, \end{aligned} \tag{2.1.47}$$

where $\vec{n}$ is the unit outward normal to A.

There are at least two important cases where the surface integral vanishes: in the first case of radiating fields (to be discussed subsequently) and in the case of quasi-state fields when $E \propto r^{-2}$ and $H \propto r^{-2}$. Since the surface of integration is proportional to r^2 at the limit $r \to \infty$ the surface integral clearly vanishes, therefore (2.1.46) reduces to

$$\int_V \vec{E}_1 \cdot \vec{J}_2 dV = \int_V \vec{E}_2 \cdot \vec{J}_1 dV. \tag{2.1.48}$$

If $\vec{J}_1$ and $\vec{J}_2$ are *infinitesimal* current elements this is to say that the variations of the electric field of the other source are negligible in the region of the source, then

$$\vec{E}_1(\mathbf{r}_2) \cdot \vec{J}_2(\mathbf{r}_2) = \vec{E}_2(\mathbf{r}_1) \cdot \vec{J}_1(\mathbf{r}_1), \tag{2.1.49}$$

which states that the field $\vec{E}_1$ produced by $\vec{J}_1$ has a component along $\vec{J}_2$ that is equal to the component along $\vec{J}_1$ of the field generated by $\vec{J}_2$ when $\vec{J}_1$ and $\vec{J}_2$ have unit magnitude. The form (2.1.48) is essentially the reciprocity principle used in circuit analysis except that $\vec{E}$ and $\vec{J}$ are replaced by the voltage V and current I.

2.2 Simple Wave Phenomena

In this section, we present solutions of the wave equation for several simple cases. A few of the examples presented here will be used subsequently to develop models which in turn enable the investigation of complex structures.

2.2.1 Simple Propagating Waves

With the source terms, constitutive relations and boundary conditions determined, one could proceed towards solution of a few simple wave phenomena. For simplicity we consider a scalar function $\psi(\mathbf{r})$ which oscillates at an angular frequency ω (i.e., we assume a steady-state regime of the form $\exp j\omega t$) and which is a solution of

$$\left[\nabla^2 + \frac{\omega^2}{c^2}\right]\psi(\mathbf{r}) = 0. \tag{2.2.1}$$

As a first stage, we examine waves propagating in *one dimension*. In a Cartesian system (x, y, z) we consider a system in which all variations are only in the z direction ($\partial/\partial x \sim 0$ and $\partial/\partial y \sim 0$), and the homogeneous wave equation reads

$$\left[\frac{\mathrm{d}^2}{\mathrm{d}z^2} + \frac{\omega^2}{c^2}\right]\psi(z) = 0. \tag{2.2.2}$$

A second order differential equation, has two solutions:

$$\psi(z) = A_+ \exp\left(-j\frac{\omega}{c}z\right) + A_- \exp\left(j\frac{\omega}{c}z\right); \tag{2.2.3}$$

these represent plane waves since the phase is constant, in the plane defined by $z = \text{const}$. The first term describes a wave propagating in the z-direction whereas the second represents a wave propagating in the opposite direction.

In a cylindrical coordinate system (r, ϕ, z), ignoring azimuthal and longitudinal variations ($\partial^2/\partial\phi^2 \sim 0$ and $\partial^2/\partial z^2 \sim 0$), the wave equation reads

$$\left[\frac{1}{r}\frac{\mathrm{d}}{\mathrm{d}r}r\frac{\mathrm{d}}{\mathrm{d}r} + \frac{\omega^2}{c^2}\right]\psi(r) = 0. \tag{2.2.4}$$

Its solution is

$$\psi(r) = A_+ \mathrm{H}_0^{(2)}\left(\frac{\omega}{c}r\right) + A_- \mathrm{H}_0^{(1)}\left(\frac{\omega}{c}r\right), \tag{2.2.5}$$

where $\mathrm{H}_0^{(1)}(\xi)$ and $\mathrm{H}_0^{(2)}(\xi)$ are the zero order Hankel function of the first and second kind; they are related to Bessel functions of the first and second kind by $\mathrm{H}_0^{(1)}(x) \equiv \mathrm{J}_0(x) + j\mathrm{Y}_0(x)$ and $\mathrm{H}_0^{(2)}(x) \equiv \mathrm{J}_0(x) - j\mathrm{Y}_0(x)$. As in the previous case, the first term represents a wave propagating from the axis outwards and the second term describes a wave propagating inwards. For completeness, we also present the solution in a spherical coordinate system (r, ϕ, θ). Ignoring all angular variations the wave equation is given by

$$\left[\frac{1}{r}\frac{\mathrm{d}^2}{\mathrm{d}r^2}r+\frac{\omega^2}{c^2}\right]\psi(r)=0, \tag{2.2.6}$$

and its solution is

$$\psi(r)=A_+\left(\frac{\omega}{c}r\right)^{-1}\exp\left(-j\frac{\omega}{c}r\right)+A_-\left(\frac{\omega}{c}r\right)^{-1}\exp\left(j\frac{\omega}{c}r\right), \tag{2.2.7}$$

where the first term represents a spherical wave propagating outwards (from the center out) whereas the second represents an inward flow.

2.2.2 The Radiation Condition

From the pure mathematical point of view, the two waves in each one of the solutions of above are a direct result of the fact that the wave equation is a second order differential equation. However, in absence of obstacles, our daily experience dictates a wave which propagates from the source outwards; this implies that in all three cases there are no "advanced" waves i.e., $A_- \equiv 0$. This is one possible interpretation of the so-called the *radiation condition* and it can be considered an additional boundary condition which is a byproduct of the causality constraint imposed on the solutions of the wave equation.

This formulation relies on the simple solutions presented above; however, the general trend is valid for solutions that are more complex. In the case of *cylindrical* azimuthally non-symmetric waves, the radiation condition implies for a solution $\psi(r,\phi,z)$, that the limit

$$\left[\psi(r,\phi,z)\exp(j\omega r/c)r^{1/2}\right]_{r\to\infty}, \tag{2.2.8}$$

is finite and it is r independent. In a similar way, for *spherical* waves described by a function $\psi(r,\phi,\theta)$, the limit

$$\left[\psi(r,\phi,\theta)\mathrm{e}^{j(\omega/c)r}r\right]_{r\to\infty}, \tag{2.2.9}$$

is finite and r independent. While this condition looks straightforward in the analytic examples presented above, it is not as trivial to impose it in numerical solvers in particular in a broad frequency range and/or when the mode configuration cannot be explicitly specified.

Wheeler and Feynman (1945) have used advanced solutions of the wave equation in order to explain the source of the so-called radiation reaction force. It is well known that electromagnetic power is emitted by a particle when it is accelerated. This power is emitted from the particle outwards and comes at the

expense of its kinetic energy. Since this change in the kinetic energy of the particle can be conceived as an effective force this is also referred to as the *radiation reaction force*.

2.2.3 Evanescent Waves

So far we have presented only waves which vary and propagate in one dimension (1D), namely solutions of the wave equation either in a Cartesian, cylindrical or spherical system of coordinate. At this point, the level of complexity is slightly elevated to include waves that vary in two dimensions. First, consider a Cartesian coordinate system in which we ignore variations in the y direction. The wave equation in this case reads

$$\left[\frac{\partial^2}{\partial x^2}+\frac{\partial^2}{\partial z^2}+\frac{\omega^2}{c^2}\right]\psi(x,z,\omega)=0, \tag{2.2.10}$$

and its formal solution, assuming a propagating behavior in the z-direction, is given by

$$\psi(x,z,\omega)=\exp(-jkz)\left[A_+\exp\left(-\sqrt{k^2-\frac{\omega^2}{c^2}}x\right)+A_-\exp\left(\sqrt{k^2-\frac{\omega^2}{c^2}}x\right)\right]. \tag{2.2.11}$$

However in the half-plane defined by $x>0$ the solution is

$$\psi(x,z,\omega)=A_+\exp(-jkz)\exp\left(-\sqrt{k^2-\frac{\omega^2}{c^2}}x\right), \tag{2.2.12}$$

since otherwise the solution diverges at $x\to\infty$. For $|k|c>\omega$ the wave decays exponentially in the x direction. This is an *evanescent wave*: it propagates in one direction and decays exponentially in another. In the opposite case, for $|k|c<\omega$, the wave propagates at an angle $\theta=\cos^{-1}(kc/\omega)$ relative to the z axis.

It is instructive to examine (2.2.12) in the time domain. Assuming zero phase for A_+ then

$$\psi(x>0,z,t)=A_+\cos(\omega t-kz)\exp\left[-\sqrt{k^2-\left(\frac{\omega}{c}\right)^2}x\right]. \tag{2.2.13}$$

Based on this expression it is convenient to introduce the concept of *phase velocity*: this is the velocity at which an imaginary observer has to move, in order to measure a constant phase $(\omega t-kz=\text{const})$; explicitly, this reads

$$\mathrm{v_{ph}} \equiv \frac{\omega}{k}. \tag{2.2.14}$$

With this definition, we observe that in a two dimensional case, an evanescent wave is characterized by a phase velocity smaller than c.

2.2.4 Waves of a Moving Charge

Evanescent waves play an important role in the interaction process of particles and waves. The simplest manifestation of their role is the representation of the spectrum of a moving charge in the laboratory frame of reference. For this purpose, we examine now the waves associated with a point charge (e) moving in the z direction at a constant velocity $\mathrm{v_0}$ in vacuum; no boundaries are involved and the system is azimuthally symmetric $(\partial/\partial\phi = 0)$. The current distribution in this case is given by

$$\mathbf{J}(\mathbf{r}, t) = -e\mathrm{v_0}\frac{1}{2\pi r}\delta(r)\delta(z - \mathrm{v_0}t)\mathbf{1}_z, \tag{2.2.15}$$

where $\mathbf{1}_z$ is a unit vector in the z direction. This current distribution excites the z component of the magnetic vector potential that in turn satisfies

$$\left[\frac{1}{r}\frac{\partial}{\partial r}r\frac{\partial}{\partial r} + \frac{\partial^2}{\partial z^2} - \frac{1}{c^2}\frac{\partial^2}{\partial t^2}\right]A_z(r, z, t) = -\mu_0 J_z(r, z, t); \tag{2.2.16}$$

its solution is assumed to have the form

$$A_z(r, z, t) = \int_{-\infty}^{\infty} \mathrm{d}\omega \exp(j\omega t)\int_{-\infty}^{\infty} \mathrm{d}k \exp(-jkz)a_z(r, k, \omega), \tag{2.2.17}$$

where $a_z(r, k, \omega)$ satisfies

$$\left[\frac{1}{r}\frac{\mathrm{d}}{\mathrm{d}r}r\frac{\mathrm{d}}{\mathrm{d}r} - \Gamma^2\right]a_z(r, k, \omega) = \frac{e\mathrm{v_0}\mu_0}{(2\pi)^2 r}\delta(r)\delta(\omega - k\mathrm{v_0}), \tag{2.2.18}$$

and $\Gamma^2 = k^2 - \omega^2/c^2$. Off-axis the solution of this equation is

$$a_z(r, k, \omega) = A_+(k, \omega)\mathrm{K_0}(\Gamma r), \tag{2.2.19}$$

where $\mathrm{K_0}(\xi)$ is the zero order modified Bessel function of the second kind. In order to determine the amplitude A_+ there are two ways to proceed: (1) calculate the azimuthal magnetic field and then impose the boundary conditions at $r = 0$. An alternative way is to (2) integrate (2.2.18) from $r = 0$ to $r = \delta \to 0$. At this point we prefer the latter primarily because this approach will be utilized extensively

subsequently. For small arguments the modified Bessel function behaves as $K_0(\xi) \simeq -\ln(\xi)$ (see Abramowitz and Stegun 1968, p. 375) and consequently,

$$A_+(k,\omega) = -\frac{e v_0 \mu_0}{(2\pi)^2}\,\delta(\omega - k v_0). \tag{2.2.20}$$

Substituting this result in (2.2.17), (2.2.19) we obtain

$$A_z(r,z,t) = -\frac{e\mu_0}{(2\pi)^2}\int_{-\infty}^{\infty} d\omega \exp\left[j\omega\left(t-\frac{z}{v_0}\right)\right] K_0\left(\frac{\omega}{c} r \frac{1}{\gamma\beta}\right), \tag{2.2.21}$$

where $\beta = v_0/c$ and $\gamma = [1-\beta^2]^{-1/2}$. Using the Lorentz gauge one can determine the scalar electric potential

$$\Phi(r,z,t) = -\frac{e}{4\pi\varepsilon_0}\frac{1}{v_0}\frac{1}{\pi}\int_{-\infty}^{\infty} d\omega \exp\left[j\omega\left(t-\frac{z}{v_0}\right)\right] K_0\left(\frac{\omega}{c} r \frac{1}{\gamma\beta}\right). \tag{2.2.22}$$

This expression indicates that the field associated with a moving charge is a superposition of cylindrical evanescent waves (for large arguments the modified Bessel function decays exponentially following $K_0(\xi) \simeq \exp(-\xi)\sqrt{\pi/2\xi}$ Abramowitz and Stegun 1968, p. 378). There is no electromagnetic *average* power emitted by this particle in the radial direction however, this average power is non-zero in the direction parallel to the particle's motion – see Exercise 2.2. When scattered by periodic structures, the evanescent waves can be "converted" into propagating waves as we shall see when the Smith-Purcell effect will be discussed in Chap. 5.

2.3 Guided Waves

In all the solutions presented above, no boundaries were involved, while in many of the topics to be considered, the electromagnetic wave is guided by either a metallic or dielectric structure. In addition to the injection of electromagnetic power into the system, metallic/dielectric structures facilitate the storage, the interaction process itself and ultimately, they allow extraction of the power out of the system.

2.3.1 Transverse Electromagnetic Mode

The simplest mode, which may develop when two metallic surfaces are present, is the *transverse electro-magnetic* (TEM) mode. In the first part of this subsection we consider the way this mode is excited. In conjunction with the electromagnetic field generated by a moving charge let us consider a *radial transmission line* consisting

of two parallel lossless plates; the distance between the plates is denoted by d and it is much smaller than the (vacuum) wavelength i.e., $\lambda(\equiv 2\pi c/\omega) \gg d$. Subject to this condition, we ignore the longitudinal variations ($\partial^2/\partial z^2 \simeq 0$) therefore, for an azimuthally symmetric system the wave equation reads

$$\left[\frac{1}{r}\frac{\mathrm{d}}{\mathrm{d}r}r\frac{\mathrm{d}}{\mathrm{d}r}+\frac{\omega^2}{c^2}\right]A_z(r,\omega) = -\mu_0 J_z(r,\omega). \tag{2.3.1}$$

An infinitely thin "wire" located on axis carries an oscillatory (ω) current, excites the magnetic vector potential; the corresponding current density is

$$J_z(r,\omega) = I\frac{1}{2\pi r}\delta(r). \tag{2.3.2}$$

Figure 2.4a illustrates schematically the system under consideration. A solution of the homogeneous wave equation, which satisfies the radiation condition, is given by

$$A_z(r,\omega) = A_+ \mathrm{H}_0^{(2)}\left(\frac{\omega}{c}r\right), \tag{2.3.3}$$

and A_+ is determined by the discontinuity at $r = 0$. Integrating (2.3.1) in the close vicinity of $r = 0$,

$$\left[r\frac{\mathrm{d}}{\mathrm{d}r}A_z(r,\omega)\right]_{r=0^+} = -\frac{\mu_0}{2\pi}I, \tag{2.3.4}$$

and using the expression for Hankel function for small arguments i.e., $\mathrm{H}_0^{(2)}(x) \simeq -j\ln(x)2/\pi$ (Abramowitz and Stegun 1968, p. 360), we obtain $A_+ = -jI\mu_0/4$.

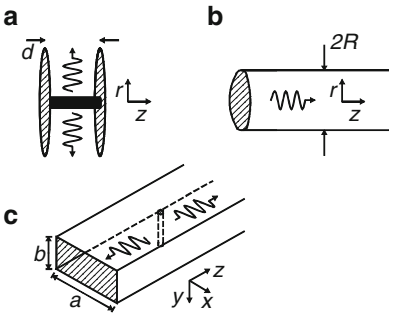

Fig. 2.4 (**a**) Propagation of transverse electro-magnetic (TEM) mode in a radial transmission line$\lambda \gg d$. (**b**) Propagation of a transverse magnetic (TM) mode in a circular waveguide – see Sect. 2.3.2. (**c**) Propagation of transverse electric (TE) mode in rectangular waveguide – Sect. 2.3.4; the curled arrows represent the direction of propagation of the waves

The corresponding longitudinal component of the electric field and the azimuthal counterpart of the magnetic field are

$$E_z(r,\omega) = -j\omega A_z(r,\omega) = -j\omega A_+ \mathrm{H}_0^{(2)}\left(\frac{\omega}{c}r\right),$$
$$H_\phi(r,\omega) = -\frac{1}{\mu_0}\frac{\mathrm{d}}{\mathrm{d}r}A_z(r,\omega) = \frac{1}{\mu_0}\frac{\omega}{c}A_+ \mathrm{H}_1^{(2)}\left(\frac{\omega}{c}r\right). \tag{2.3.5}$$

With these two components, the radial component of the Poynting vector is

$$S_r(r) = -\frac{1}{2}E_z(r)H_\phi^*(r), \tag{2.3.6}$$

and consequently, the total power radiated is

$$P = \mathrm{Re}[2\pi r d S_r(r)] = \frac{1}{8}\left(\frac{\omega}{c}d\right)\eta_0 I^2. \tag{2.3.7}$$

In the last expression, we used the asymptotic approximation for large arguments of Hankel function i.e., $\mathrm{H}_0^{(2)}(x) \simeq \exp(-jx)\sqrt{2/\pi x}$ (see Abramowitz and Stegun 1968, p. 364). Bearing mind that in steady state the average power dissipated on a resistor carrying a current I is $P = RI^2/2$, the impedance associated with the radiation process is

$$R_{\mathrm{rad,TEM}} \equiv \frac{P}{I^2/2} = \frac{1}{4}\eta_0\left(\frac{\omega}{c}d\right); \tag{2.3.8}$$

in this expression $\eta_0 \equiv \sqrt{\mu_0/\varepsilon_0}$ is the *vacuum impedance* of a plane wave. At 9 GHz and for $d = 5\,\mathrm{mm}$ the impedance is $90[\Omega]$ which is 5 times larger (for the same parameters) than the radiation impedance in free-space defined as $R_{\mathrm{rad}} = \eta_0(\omega d/c)^2/6\pi \sim 18[\Omega]$. The radiation impedance is a measure, extensively used in antenna theory, which represents the effect of the surroundings on the radiation emitted by a source.

2.3.2 Transverse Magnetic Mode

Transverse magnetic (TM) modes can develop in the radial system discussed previously and their characteristics will be further investigated in Chap. 4, in the context of periodic structures. Here we review the characteristics of these modes for a circular cylindrical waveguide of radius R filled with a dielectric material of relative permittivity ε_r; the relative permeability is taken to unity ($\mu_r = 1$). We assume that the walls of the waveguide are made of an ideal conducting material ($\sigma \to \infty$) therefore, the tangential electric field at the walls vanishes. To this

configuration, a cylindrical system of coordinates (r, ϕ, z) is attached – see Fig. 2.4b and the waves are assumed to be excited by an *azimuthally symmetric* source therefore we may take $\partial/\partial\phi = 0$.

The electromagnetic field in the waveguide has two contributions. One is from the z component of the magnetic vector potential

$$A_z(r, z, \omega) = \sum_{s=1}^{\infty} A_s \mathrm{J}_0\left(p_s \frac{r}{R}\right) \mathrm{e}^{-\Gamma_s z}, \tag{2.3.9}$$

where

$$\Gamma_s^2 = \frac{p_s^2}{R^2} - \varepsilon_\mathrm{r} \frac{\omega^2}{c^2}, \tag{2.3.10}$$

$\mathrm{J}_0(\xi)$ is the zero order Bessel function of the first kind and p_s are the zeros of this function ($p_1 = 2.4048, p_2 = 5.52\ldots$). The second, is from the scalar electric potential Φ

$$\Phi(r, z, \omega) = \sum_{s=1}^{\infty} \Phi_s \mathrm{J}_0\left(p_s \frac{r}{R}\right) \mathrm{e}^{-\Gamma_s z}. \tag{2.3.11}$$

Lorentz gauge (2.1.38) correlates the two amplitudes, namely

$$\Phi_s = \frac{c^2 \Gamma_s}{j\omega\varepsilon_\mathrm{r}} A_s. \tag{2.3.12}$$

In this solution, the waves are assumed to propagate from the source without obstacles thus no reflected waves were included.

The three non-trivial components of the electromagnetic field are: the azimuthal magnetic field

$$H_\phi = -\frac{1}{\mu_0} \frac{\partial A_z}{\partial r} = \frac{1}{\mu_0} \sum_{s=1}^{\infty} A_s \frac{p_s}{R} \mathrm{J}_1\left(p_s \frac{r}{R}\right) \mathrm{e}^{-\Gamma_s z} \tag{2.3.13}$$

the radial electric field

$$E_r = -\frac{\partial \Phi}{\partial r} = \sum_{s=1}^{\infty} A_s \frac{c^2 \Gamma_s}{j\omega\varepsilon_\mathrm{r}} \frac{p_s}{R} \mathrm{J}_1\left(p_s \frac{r}{R}\right) \mathrm{e}^{-\Gamma_s z}, \tag{2.3.14}$$

and the longitudinal electric field

$$E_z = -\frac{\partial \Phi}{\partial z} - j\omega A_z = \sum_{s=1}^{\infty} A_s \frac{c^2}{j\omega\varepsilon_\mathrm{r}} \left(\frac{p_s}{R}\right)^2 \mathrm{J}_0\left(p_s \frac{r}{R}\right) \mathrm{e}^{-\Gamma_s z} \tag{2.3.15}$$

With the electromagnetic field determined, the average magnetic and electric energy per unit length can be calculated. These are given by

$$\begin{aligned} W_{\mathrm{M}} &= \frac{1}{4}\mu_0 2\pi \int_0^R \mathrm{d}r r|H_\phi|^2 = \frac{\pi}{2\mu_0}\sum_{s=1}^{\infty}|A_s|^2\frac{p_s^2}{R^2}\left[\frac{R^2}{2}\mathrm{J}_1^2(p_s)\right]\mathrm{e}^{-(\Gamma_s+\Gamma_s^*)z}, \\ W_{\mathrm{E}} &= \frac{1}{4}\varepsilon_0\varepsilon_{\mathrm{r}} 2\pi \int_0^R \mathrm{d}r r\left[|E_r|^2+|E_z|^2\right] \\ &= \frac{\pi}{2}\varepsilon_0\varepsilon_{\mathrm{r}}\sum_{s=1}^{\infty}|A_s|^2\left[\frac{c^4}{\omega^2\varepsilon_{\mathrm{r}}^2}\frac{p_s^2}{R^2}\right]\left[\Gamma_s\Gamma_s^*+\frac{p_s^2}{R^2}\right]\left[\frac{R^2}{2}\mathrm{J}_1^2(p_s)\right]\mathrm{e}^{-(\Gamma_s+\Gamma_s^*)z} \end{aligned} \tag{2.3.16}$$

In these expressions the orthogonality of the Bessel functions was used i.e.,

$$\int_0^R \mathrm{d}r r\mathrm{J}_0\left(p_s\frac{r}{R}\right)\mathrm{J}_0\left(p_{s'}\frac{r}{R}\right) = \frac{1}{2}R^2\mathrm{J}_1^2(p_s)\delta_{s,s'}. \tag{2.3.17}$$

In a similar way, we can determine the total average power that flows in the waveguide:

$$\begin{aligned} P &= \mathrm{Re}\left[2\pi\int_0^R \mathrm{d}r r\frac{1}{2}E_r H_\phi^*\right] \\ &= \frac{\pi}{\mu_0}\sum_{s=1}^{\infty}|A_s|^2\frac{p_s^2}{R^2}\left[\frac{R^2}{2}\mathrm{J}_1^2(p_s)\right]\mathrm{Re}\left[\mathrm{e}^{-\left(\Gamma_S+\Gamma_S^*\right)z}\frac{c^2\Gamma_s}{j\omega\varepsilon_{\mathrm{r}}}\right]. \end{aligned} \tag{2.3.18}$$

According to this expression, we observe that power is carried along the waveguide only by the propagating modes namely those which satisfy

$$\Gamma_s^2 = \frac{p_s^2}{R^2} - \varepsilon_{\mathrm{r}}\frac{\omega^2}{c^2} < 0. \tag{2.3.19}$$

The remainders are below cut-off and they do not carry any (real) power. The situation is different when reflections are present.

2.3.3 Velocities and Impedances

Energy Velocity. In the context of power-flow presented above it is convenient to define several parameters that help to characterize the interaction of waves and electron beams in various configurations. For a relatively narrow band signal, the energy velocity is a measure of the power flow in the system relative to the total energy stored per unit length namely,

$$\mathrm{v}_{\mathrm{en}} = \frac{P}{W_{\mathrm{M}} + W_{\mathrm{E}}}. \tag{2.3.20}$$

In a circular cylindrical waveguide with a single propagating mode ($s = 1$), the energy velocity reads

$$\mathrm{v}_{\mathrm{en}} = c\frac{1}{\varepsilon_{\mathrm{r}}}\sqrt{\varepsilon_{\mathrm{r}} - \left(\frac{p_1 c}{\omega R}\right)^2}. \tag{2.3.21}$$

From the definition of the energy velocity (2.3.20) it is evident that whenever more than one mode propagates in the waveguide the energy velocity is dependent on the *relative* amplitudes of the various modes. Another point which should be emphasized since it will be encountered again later in this text is the fact that even if only one mode propagates and there is a substantial amount of energy stored in the higher non-propagating modes, the energy velocity will be much slower than indicated by the expression in (2.3.21).

Phase Velocity. A general definition of this quantity was introduced in Sect. 2.2.3 (2.2.14). In a cylindrical waveguide with no dielectric, the phase velocity is always larger than c. However if $\varepsilon_{\mathrm{r}} > 1 + (p_1 c/\omega R)^2$ the phase velocity is smaller than c. In fact, for high frequencies ($\omega R/c \gg p_1$) the phase velocity is determined entirely by the medium: $\mathrm{v}_{\mathrm{ph}} \sim c/\sqrt{\varepsilon_{\mathrm{r}}}$.

Group Velocity. This is a kinematical quantity indicative of the propagation of a relatively smooth spectrum of waves. To envision the meaning of the group velocity, imagine that a system is fed by two waves oscillating at adjacent frequencies $\omega_1 = \omega + \Delta\omega$, $\omega_2 = \omega - \Delta\omega$ having the form

$$f(z,t) = \cos(\omega_1 t - K_1 z) + \cos(\omega_2 t - K_2 z), \tag{2.3.22}$$

where the wave-numbers $K_1 = k + \Delta k$, $K_2 = k - \Delta k$ are the corresponding wave-numbers with $k = \sqrt{(\omega/c)^2 - (p_1/R)^2}$. Explicitly we can now write the expression in (2.3.22) as

$$f(z,t) = 2\cos(\Delta\omega t - \Delta k z)\cos(\omega t - k z). \tag{2.3.23}$$

Assuming that $|\Delta\omega| \ll \omega$, we can consider the first trigonometric function as a slow varying amplitude. As such, we can ask what has to be the velocity of an observer in order to experience a constant *amplitude* i.e., $\Delta\omega\delta t - \Delta k\delta z = 0$; in this case, the answer will be $\mathrm{v}_{\mathrm{gr}} \equiv \frac{\Delta\omega}{\Delta k}$ or at the limit of $\Delta\omega \to 0$,

$$\mathrm{v}_{\mathrm{gr}} \equiv \frac{\partial\omega}{\partial k}. \tag{2.3.24}$$

If the dielectric coefficient is not frequency dependent, the group velocity of a propagating TM mode is $\mathrm{v}_{\mathrm{gr}} = c^2 k/\omega\varepsilon_{\mathrm{r}}$ and it satisfies

$$\mathrm{v_{gr}v_{ph}} = \frac{c^2}{\varepsilon_r}. \tag{2.3.25}$$

Although this relation is valid only for uniformly filled waveguide it provides information about the general trend in the variation of the group velocity as the (effective) dielectric coefficient changes in partially loaded systems.

Characteristic Impedance. There are several kinds of impedances that can be defined. Two of which will be defined here and a third one, will be defined in Chap. 8. The first is basically oriented towards the propagation of the electromagnetic mode in the structure and this is the characteristic impedance which is the ratio between the two transverse components of the field, E_r and H_ϕ, it reads

$$Z_{\mathrm{ch}} \equiv \frac{E_r}{H_\phi} = \eta_0 \frac{c\Gamma_s}{j\omega\varepsilon_{\mathrm{r}}}. \tag{2.3.26}$$

Interaction Impedance. The second impedance is indicative of the electric field which a *thin* pencil or annular beam experiences as it traverses the waveguide. For this purpose, we define the effective longitudinal electric field in the region where the electron beam will be injected. For a pencil beam ($0 \leq r \leq R_{\mathrm{b}}$) this is given by

$$|E(z)|^2 \equiv \frac{2}{R_b^2} \int_0^{R_{\mathrm{b}}} \mathrm{d}r r |E_z(r,z,\omega)|^2, \tag{2.3.27}$$

whereas for an annular beam ($R_{\mathrm{b}} - \Delta/2 \leqslant r \leqslant R_{\mathrm{b}} + \Delta/2$) it reads

$$|E(z)|^2 \equiv \frac{1}{\Delta R_{\mathrm{b}}} \int_{R_{\mathrm{b}}-\Delta/2}^{R_{\mathrm{b}}+\Delta/2} \mathrm{d}r r |E_z(r,z,\omega)|^2. \tag{2.3.28}$$

For either one of the cases we define the interaction impedance as

$$Z_{\mathrm{int}} \equiv \frac{1}{2}|E(z)|^2 \pi R^2 \frac{1}{P(z)}. \tag{2.3.29}$$

Note that although we are motivated by the presence of a beam of electrons, all the quantities in the definition of the interaction impedance are "cold" quantities namely, they do not account for the presence of the beam. It should be pointed out that the definition introduced here differs from Pierce's [Pierce (1947)] definition, $Z_{\mathrm{int}} = |E|^2/2k^2P$ by the factor k^2 which was replaced by the inverse of the area where the wave propagates, $1/\pi R^2$. This definition is in particular useful in tapered structures where the internal radius of the system is kept constant but the other geometric parameters may vary in space such that the phase velocity varies.

For our particular system the interaction impedance reads

$$Z_{\mathrm{int}} = \eta_0 \left[\frac{p_1}{\varepsilon_r}\frac{c}{\omega R}\right]^2 \frac{\mathrm{J}_0^2(p_1 R_{\mathrm{b}}/R) + \mathrm{J}_1^2(p_1 R_{\mathrm{b}}/R)}{\mathrm{J}_1^2(p_1)} \frac{1}{\beta_{\mathrm{en}}}; \tag{2.3.30}$$

here $\beta_{en} = v_{en}/c$ is the normalized energy velocity which in many cases is equal or close to the group velocity (in this particular case it is equal). One may expect to achieve maximum efficiency when the longitudinal electric field $[E(z)]$ experienced by the electron is maximum. Therefore, according to the definition in (2.3.29), from the point of view of the beam-wave interaction, the purpose should be to design a structure with the highest interaction impedance. According to (2.3.30) there are three possibilities: (1) operate at low frequency, which in many cases is not desirable, (2) have a structure with small radius which might be acceptable or (3) design a structure with low energy (group) velocity. It should be pointed out that these three possibilities are interdependent since for example, the energy velocity depends on both frequency and radius. One possibility to design a low group velocity structure is to have a small radius.

Interaction Dielectric Coefficient. This quantity is indicative of the total average electromagnetic energy stored per unit length in terms of the longitudinal component of the electric field experienced by a thin annular/pencil beam:

$$\varepsilon_{int} \equiv W(z)\left[\frac{1}{2}\varepsilon_0|E(z)|^2\pi R^2\right]^{-1}. \tag{2.3.31}$$

In our particular case it reads

$$\varepsilon_{int} = \left[\frac{\varepsilon_r}{p_1}\frac{\omega}{c}R\right]^2 \frac{J_1^2(p_1)}{J_0^2(p_1 R_b/R) + J_1^2(p_1 R_b/R)}. \tag{2.3.32}$$

Note that according to the definitions of the interaction impedance (2.3.29) and the effective dielectric coefficient (2.3.31) their product is inversely proportional to the energy velocity:

$$Z_{int}\varepsilon_{int} = \eta_0 \frac{1}{\beta_{en}}. \tag{2.3.33}$$

Since the definitions above (2.3.29) and (2.3.31) are general, as long as there is only one dominant mode in the system, the result in the last expression is also general.

2.3.4 Transverse Electric Mode

In many cases, electromagnetic power is transferred along a waveguide in the transverse electric (TE) mode due to its low loss (Ramo et al. 1965, p. 424). In many devices, power is extracted using rectangular waveguides, therefore we consider next the characteristics of such a waveguide. In Sect. 2.3.1 we examined the radiation emitted from a dipole oscillating in azimuthally symmetric radial

transmission line. In this geometry, the main mode generated was the transverse electro-magnetic (TEM) mode. In this section, we consider the same problem in a rectangular waveguide whose wide dimension is a and the narrow one is b – see Fig. 2.4c. Variations along the narrow dimension are neglected ($\partial/\partial y \sim 0$). An infinitesimally thin "wire" (dipole) is located in the center of the waveguide and it prescribes a current density given by

$$J_y(x,z,\omega) = I\delta\left(x-\frac{a}{2}\right)\delta(z). \tag{2.3.34}$$

It excites the transverse electric field $E_y(x,z,\omega)$ that satisfies

$$\left[\frac{\partial^2}{\partial x^2}+\frac{\partial^2}{\partial z^2}+\frac{\omega^2}{c^2}\right]E_y(x,z,\omega) = j\omega\mu_0 J_y(x,z,\omega), \tag{2.3.35}$$

subject to the boundary conditions: $E_y(x=0,z,\omega)=0$ and $E_y(x=a,z,\omega)=0$. The solution can be represented as a superposition of trigonometric functions i.e.,

$$E_y(x,z,\omega) = \sum_{n=1}^{\infty} E_n(z,\omega)\sin\left(\frac{\pi n}{a}x\right), \tag{2.3.36}$$

where $E_n(z,\omega)$ satisfies

$$\left[\frac{\mathrm{d}^2}{\mathrm{d}z^2}-\left(\frac{\pi n}{a}\right)^2+\frac{\omega^2}{c^2}\right]E_n(z,\omega) = j\omega\mu_0 I\sin\left(\frac{\pi}{2}n\right)\frac{2}{a}\delta(z) \equiv I_n\delta(z). \tag{2.3.37}$$

For $z>0$ the solution of this equation is

$$E_n(z>0) = A_+ \mathrm{e}^{-\Gamma_n z}, \tag{2.3.38}$$

and for $z<0$

$$E_n(z<0) = A_- \mathrm{e}^{\Gamma_n z}, \tag{2.3.39}$$

where $\Gamma_n^2 = (\pi n/a)^2 - (\omega/c)^2$. The transverse electric field has to be continuous at $z=0$ thus

$$A_+ = A_-, \tag{2.3.40}$$

whereas its derivative is discontinuous. The discontinuity is determined by the Dirac delta function in (2.3.37) therefore by integrating the latter we obtain

$$\left[\frac{\mathrm{d}}{\mathrm{d}z}E_n(z)\right]_{z=0^+} - \left[\frac{\mathrm{d}}{\mathrm{d}z}E_n(z)\right]_{z=0^-} = I_n, \tag{2.3.41}$$

hence

$$-\Gamma_n A_+ - \Gamma_n A_- = I_n. \tag{2.3.42}$$

From (2.3.40), (2.3.42) we conclude that the transverse electric field reads

$$E_y(x,z,\omega) = -\sum_{n=1}^{\infty} \frac{I_n}{2\Gamma_n} \mathrm{e}^{-\Gamma_n|z|} \sin\left(\frac{\pi n}{a}x\right). \tag{2.3.43}$$

As in Sect. 2.3.1 we next calculate the power generated by the current distribution in (2.3.34). For this purpose the transverse magnetic field is calculated since it is the only component which contributes to the longitudinal component of the Poynting vector; H_x for $z>0$ reads

$$H_x(x,z>0,\omega) = -\sum_{n=1}^{\infty} \frac{\Gamma_n}{j\omega\mu_0} \frac{I_n}{2\Gamma_n} \mathrm{e}^{-\Gamma_n z} \sin\left(\frac{\pi n}{a}x\right). \tag{2.3.44}$$

Before proceeding note that similar to the transverse magnetic mode, the phase velocity (for $\omega > \pi nc/a$ and $\varepsilon_\mathrm{r} = 1$) is always larger than c. Nevertheless, the characteristic impedance (in vacuum) of the nth propagating mode,

$$Z_{\mathrm{ch,TE}} \equiv \frac{E_y}{H_x} = \frac{j\omega\mu_0}{\Gamma_n} \tag{2.3.45}$$

is always larger than the vacuum impedance (η_0), in contrast to the TM mode, where the characteristic impedance is always smaller than η_0.

Now we can focus our attention to the power flow: the average power which flows in the positive z direction, assuming a single mode above cut-off, is given by

$$P_+ = \frac{1}{2} \frac{I_1}{2\sqrt{(\omega/c)^2 - (\pi/a)^2}} \frac{I_1^*}{2\omega\mu_0} \frac{1}{2} ab. \tag{2.3.46}$$

The radiation impedance is determined by the power emitted in both directions divided by $\frac{1}{2}|I|^2$ and it reads

$$R_{\mathrm{rad,TE}} \equiv \frac{P_+ + P_-}{\frac{1}{2}|I|^2} = \eta_0 \frac{\omega b/c}{\sqrt{(\omega a/c)^2 - \pi^2}} = \frac{b}{a} Z_{\mathrm{ch,TE}}. \tag{2.3.47}$$

At 9 GHz, and for $a = 2.5\,\mathrm{cm}$, $b = 0.5\,\mathrm{cm}$, this impedance is $100\,\Omega$ which is close to that calculated in the case of the radial transmission line as calculated in Sect. 2.3.1.

2.3.5 TE, TM and Hybrid Modes in a Dielectric Waveguide

Pure TM or TE modes are possible only in a limited set of geometries. In most cases these modes are coupled and in this section we present a well-known configuration that supports either TE, TM or hybrid modes – this is the dielectric waveguide. In its simplest configuration it consists of a dielectric (ε_r) fiber of radius R. For small-diameter rods, the field extends for a considerable distance beyond the surface, and the axial propagation constant k_z is only slightly larger than ω/c. At the limit of an infinite radius $k_z = \omega\sqrt{\varepsilon_r}/c$. The field components, omitting the term $\exp(-jn\phi - j\beta z)$, are determined in Table 2.1; $\Lambda^2 = \varepsilon_r\omega^2/c^2 - k_z^2$ and $\Gamma^2 = k_z^2 - \omega^2/c^2$; the prime indicates differentiation with respect to the arguments of the corresponding Bessel functions.

Imposing of the boundary conditions at $r = R$ leads to the dispersion relation

$$\left[\frac{\varepsilon J'_n(a)}{aJ_n(a)} - \frac{K'_n(b)}{bK_n(b)}\right]\left[\frac{J'_n(a)}{aJ_n(a)} + \frac{K'_n(b)}{bK_n(b)}\right] = \left[n\frac{ck_z}{\omega}\,\frac{(b^2+a^2)}{a^2b^2}\right]^2 \tag{2.3.48}$$

where $a = \Lambda R$, $b = \Gamma R$. When $n = 0$, the right-hand side vanishes, and each factor on the left-hand side must equal zero. These two terms determine the dispersion of the axially symmetric TM and TE modes:

$$\begin{aligned} &\text{TM modes}: \quad \frac{\varepsilon_r J'_0(a)}{aJ_0(a)} = \frac{K'_0(b)}{bK_0(b)} \\ &\text{TE modes}: \quad \frac{J'_0(a)}{aJ_0(a)} = -\frac{K'_0(b)}{bK_0(b)}. \end{aligned} \tag{2.3.49}$$

Based on their definitions, a and b are related by $a^2 + b^2 = (\varepsilon_r - 1)(\omega R/c)^2$. Clearly, pure TM or TE modes are possible only if the field is independent of the azimuthal coordinate ϕ namely, $n = 0$. As the radius of the rod increases, the number of TM and TE modes also increases. All modes with angular dependence are a combination of a TM and a TE mode, and are classified as hybrid modes.

Table 2.1 Field components in a cylindrical dielectric waveguide

$r < R$	$r > R$
$E_z = A_n J_n(\Lambda r)$	$E_z = C_n K_n(\Gamma r)$
$E_r = -\frac{jk_z}{\Lambda}A_n J'_n - \frac{n\omega\mu_0}{\Lambda^2 r}B_n J_n$	$E_r = \frac{jk_z}{\Gamma}C_n K'_n + \frac{n\omega\mu_0}{\Gamma^2 r}D_n K_n$
$E_\phi = -\frac{nk_z}{\Lambda^2 r}A_n J_n + \frac{j\omega\mu_0}{\Lambda}B_n J'_n$	$E_\phi = -\frac{nk_z}{\Gamma^2 r}C_n K_n - \frac{j\omega\mu_0}{\Gamma}D_n K'_n$
$H_z = B_n J_n(\Lambda r)$	$H_z = D_n K_n(\Gamma r)$
$H_r = \frac{n\omega\varepsilon}{\Lambda^2 r}A_n J_n - \frac{jk_z}{\Lambda}B_n J'_n$	$H_r = -\frac{n\omega\varepsilon_0}{\Gamma^2 r}C_n K_n - \frac{jk_z}{\Gamma}D_n K'_n$
$H_\phi = -\frac{j\omega\varepsilon}{\Lambda}A_n J'_n - \frac{nk_z}{\Lambda^2 r}B_n J_n$	$H_\phi = \frac{j\omega\varepsilon_0}{\Gamma}C_n K'_n + \frac{nk_z}{\Gamma^2 r}D_n K_n$

Comment 2.4. Contrary to metallic waveguide the HE_{11} mode, for example, has no low-frequency cutoff.

2.4 Green's Scalar Theorem

Green's function is a useful tool for calculation of electromagnetic field generated by a distributed source (particles) subject to the boundary conditions imposed by the structure. The logic behind the method presented below is the following: instead of solving for an arbitrary source we solve for a point source and by virtue of the linearity of Maxwell's equations, the field at a given location is a *superposition* of all the point sources that constitute the real source.

Let us assume that we have to solve the non-homogeneous wave equation:

$$\left[\nabla^2 + \frac{\omega^2}{c^2}\right]\psi(\mathbf{r}) = -s(\mathbf{r}), \tag{2.4.1}$$

where $s(\mathbf{r})$ is an arbitrary source which is assumed to be known. Instead of solving this equation let us assume for the moment that we know how to solve a simpler problem namely,

$$\left[\nabla^2 + \frac{\omega^2}{c^2}\right]G(\mathbf{r}|\mathbf{r}') = -\delta(\mathbf{r} - \mathbf{r}'), \tag{2.4.2}$$

where the coefficient of the Dirac delta function on the right-hand side was chosen such that the result of the integration over the entire space is unity. We can then multiply (2.4.1) by $G(\mathbf{r}|\mathbf{r}')$ and (2.4.2) by $\psi(\mathbf{r}')$, subtract the two results to obtain

$$G(\mathbf{r}|\mathbf{r}')\nabla^2\psi(\mathbf{r}') - \psi(\mathbf{r}')\nabla^2 G(\mathbf{r}|\mathbf{r}') = -G(\mathbf{r}|\mathbf{r}')s(\mathbf{r}') + \psi(\mathbf{r}')\delta(\mathbf{r} - \mathbf{r}'). \tag{2.4.3}$$

Integrating over the entire and using Gauss' theorem, we get

$$\psi(\mathbf{r}) = \int_V \mathrm{d}V' G(\mathbf{r}|\mathbf{r}')s(\mathbf{r}') + \oiint \mathrm{d}\mathbf{a}' \cdot [G(\mathbf{r}|\mathbf{r}')\nabla'\psi(\mathbf{r}') - \psi(\mathbf{r}')\nabla' G(\mathbf{r}|\mathbf{r}')]; \tag{2.4.4}$$

$\oiint$ is a surface integral which encloses the volume V. This is the scalar Green's theorem. In free space Green's theorem reads

$$\psi(\mathbf{r}) = \int_V \mathrm{d}V' G(\mathbf{r}|\mathbf{r}')s(\mathbf{r}'). \tag{2.4.5}$$

Next, we employ Green's theorem for the calculation of the Cerenkov effect in two cases: firstly, in a boundless system and secondly in a waveguide.

2.4.1 Cerenkov Radiation in the Boundless Case

Let us examine the electromagnetic field generated by a charge (e) as it moves in gas a medium which is characterized by a dielectric coefficient larger than unity, $\varepsilon_r > 1$; its velocity is v. For simplicity sake, it will be assumed that the dielectric coefficient is frequency-independent.

A current density described by the same expression as in (2.2.15) drives the system and for an azimuthally symmetric medium the wave equation is

$$\left[\frac{1}{r}\frac{\partial}{\partial r}r\frac{\partial}{\partial r}+\frac{\partial^2}{\partial z^2}-\varepsilon_r\frac{1}{c^2}\frac{\partial^2}{\partial t^2}\right]A_z(r,z,t)=-\mu_0 J_z(r,z,t); \tag{2.4.6}$$

the other two components of the magnetic vector potential are zero and the electric scalar potential can be determined using Lorentz gauge. The time Fourier transform of the magnetic vector potential is defined by

$$A_z(r,z,t)=\int_{-\infty}^{\infty}\mathrm{d}\omega \mathrm{e}^{j\omega t}A_z(r,z,\omega), \tag{2.4.7}$$

where $A_z(r,z,\omega)$ satisfies

$$\left[\frac{1}{r}\frac{\partial}{\partial r}r\frac{\partial}{\partial r}+\frac{\partial^2}{\partial z^2}+\varepsilon_r\frac{\omega^2}{c^2}\right]A_z(r,z,\omega)=-\mu_0 J_z(r,z,\omega), \tag{2.4.8}$$

and the time Fourier transform of the current density in (2.2.15) is

$$J_z(r,z,\omega)=-\frac{e}{(2\pi)^2 r}\delta(r)\exp\left(-j\frac{\omega}{\mathrm{v}}z\right). \tag{2.4.9}$$

Green's function associated with this problem is a solution of

$$\left[\frac{1}{r}\frac{\partial}{\partial r}r\frac{\partial}{\partial r}+\frac{\partial^2}{\partial z^2}+\varepsilon_r\frac{\omega^2}{c^2}\right]G(r,z|r',z')=\frac{-1}{2\pi r}\delta(r-r')\delta(z-z') \tag{2.4.10}$$

which can be represented by

$$G(r,z|r',z')=\int_{-\infty}^{\infty}\mathrm{d}k g_k(r|r')\exp[-jk(z-z')], \tag{2.4.11}$$

and $g_k(r|r')$ satisfies

$$\left[\frac{1}{r}\frac{\mathrm{d}}{\mathrm{d}r}r\frac{\mathrm{d}}{\mathrm{d}r}-\Gamma^2\right]g_k(r|r')=-\frac{1}{(2\pi)^2 r}\delta(r-r'), \tag{2.4.12}$$

where

$$\Gamma^2 = k^2 - \varepsilon_\mathrm{r}\frac{\omega^2}{c^2}. \tag{2.4.13}$$

The solution of this equation for $r > r' > 0$ is

$$g_k(r|r' < r) = F_1(r')\mathrm{K}_0(\Gamma r), \tag{2.4.14}$$

and for $r' > r > 0$ it reads

$$g_k(r < r'|r') = F_2(r')\mathrm{I}_0(\Gamma r). \tag{2.4.15}$$

The function $g_k(r|r')$ has to be continuous at $r = r'$ i.e.,

$$F_1(r')\mathrm{K}_0(\Gamma r') = F_2(r')\mathrm{I}_0(\Gamma r'), \tag{2.4.16}$$

whereas its derivative is discontinuous at the same location. To determine the discontinuity we integrate (2.4.12)

$$\left[r\frac{\mathrm{d}}{\mathrm{d}r}g(r|r')\right]_{r=r'+0} - \left[r\frac{\mathrm{d}}{\mathrm{d}r}g(r|r')\right]_{r=r'-0} = -\frac{1}{(2\pi)^2}, \tag{2.4.17}$$

hence

$$-r'F_1(r')\Gamma\mathrm{K}_1(\Gamma r') - r'F_2(r')\Gamma\mathrm{I}_1(\Gamma r') = -\frac{1}{(2\pi)^2}. \tag{2.4.18}$$

From (2.4.16), (2.4.18) and using the fact that $\mathrm{K}_0(\xi)\mathrm{I}_1(\xi) + \mathrm{K}_1(\xi)\mathrm{I}_0(\xi) = 1/\xi$ (see Abramowitz and Stegun 1968, p. 375) we finally obtain

$$g_k(r|r') = \frac{1}{(2\pi)^2}\begin{cases} \mathrm{I}_0(\Gamma r)\mathrm{K}_0(\Gamma r') & \text{for} \quad 0 \le r \le r' < \infty, \\ \mathrm{K}_0(\Gamma r)\mathrm{I}_0(\Gamma r') & \text{for} \quad 0 \le r' \le r < \infty. \end{cases} \tag{2.4.19}$$

This expression together with (2.4.11) determine Green's function in a boundless space.

With this function, Green's theorem (2.4.5) and the current density as given in (2.4.9), we can determine the magnetic vector potential. It reads

$$A_z(r, z, \omega) = -\frac{e\mu_0}{(2\pi)^2}\mathrm{K}_0\left(\frac{\omega}{c}r\sqrt{\beta^{-2} - n^2}\right)\exp\left(-j\frac{\omega}{\mathrm{v}}z\right), \tag{2.4.20}$$

where $n \equiv \sqrt{\varepsilon_\mathrm{r}}$ is the refractive index of the medium. If we examine this solution far away from the source and use the asymptotic value for large arguments

$\left[(\omega/c)r|\sqrt{\beta^{-2}-n^2}| \gg 1\right]$ of the modified Bessel function, the magnetic vector potential reads

$$A_z(r,z,\omega) \propto \exp\left(-\frac{\omega}{c}r\sqrt{\beta^{-2}-n^2}\right)\exp\left(-j\frac{\omega}{\mathrm{v}}z\right). \tag{2.4.21}$$

If n is smaller than $1/\beta$ the field decays exponentially in the radial direction since, as in vacuum, this is an *evanescent* wave.

When the velocity of the particle, $\mathrm{v} = \beta c$, is larger than the phase velocity of a plane wave in the medium (c/n) i.e., $\beta > 1/n$, the expression above represents a *propagating* wave – this is called Cerenkov radiation. The emitted wave is not parallel to the electron's trajectory but it propagates at an angle θ relative to this direction (z axis) given by

$$k_z = \frac{\omega}{c}n\cos\theta = \frac{\omega}{c}\frac{1}{\beta} \tag{2.4.22}$$

This determines what it is known as the Cerenkov radiation angle, θ_c

$$\theta_c = \cos^{-1}\left(\frac{1}{n\beta}\right). \tag{2.4.23}$$

Since the phase velocity of the wave is smaller than that of the particle, clearly, the radiation lags behind the particle. This fact will become evident in the next subsection. However, before proceeding, it is important to make a comment regarding Cerenkov radiation emitted by a single particle and an *ensemble* of N electrons: by virtue of the linearity of Maxwell's equation the total field is a superposition of the contributions of all electrons. For wavelengths significantly *longer* than the bunch-length, the various contributions add up coherently and since the power is proportional to the square of the field, the emitted power is proportional to the square of the number of electrons ($P \propto N^2$) – this is also referred to as *coherent radiation*. For wavelengths *shorter* than the bunch, the average field vanishes therefore, the total power is a product of the power emitted by a single electron and the number of electrons. The proof is left to the reader and the details are phrased as an Exercise 2.7 at the end of this chapter.

2.4.2 Cerenkov Radiation in a Cylindrical Waveguide

In this subsection we consider the electromagnetic field associated with the symmetric transverse magnetic (TM) mode in a *dielectric* filled waveguide. As in the previous subsection, the source of this field is a particle moving at a velocity v, however, the main difference is that the solution has a constraint since on the

waveguide's wall $(r = R)$ the tangential electric field vanishes. Therefore, we calculate Green's function subject to the condition $G(r = R, z|r', z') = 0$. We assume a solution of the form

$$G(r, z|r', z') = \sum_{s=1}^{\infty} G_s(z|r', z') \mathrm{J}_0\left(p_s \frac{r}{R}\right), \tag{2.4.24}$$

substitute in (2.4.10) and use the orthogonality of the Bessel functions we find that

$$G_s(z|r', z') = \mathrm{J}_0\left(p_s \frac{r'}{R}\right) \frac{1}{\frac{1}{2}R^2 \mathrm{J}_1^2(p_s)} g_s(z|z'), \tag{2.4.25}$$

where $g_s(z|z')$ satisfies

$$\left[\frac{\mathrm{d}^2}{\mathrm{d}z^2} - \Gamma_s^2\right] g_s(z|z') = -\frac{1}{2\pi}\delta(z - z'), \tag{2.4.26}$$

and $\Gamma_s^2 = p_s^2/R^2 - \varepsilon_{\mathrm{r}}\omega^2/c^2$. For $z > z'$ the solution of (2.4.26) is

$$g_s(z|z') = A_+ \mathrm{e}^{-\Gamma_s(z-z')}, \tag{2.4.27}$$

and for $z < z'$ the solution is

$$g_s(z|z') = A_- \mathrm{e}^{\Gamma_s(z-z')}. \tag{2.4.28}$$

Green's function is continuous at $z = z'$ i.e.,

$$A_+ = A_-, \tag{2.4.29}$$

and its first derivative is discontinuous. The discontinuity is determined by integrating (2.4.26) from $z = z' - 0$ to $z = z' + 0$ i.e.,

$$\left[\frac{\mathrm{d}}{\mathrm{d}z} g_s(z|z')\right]_{z=z'+0} - \left[\frac{\mathrm{d}}{\mathrm{d}z} g_s(z|z')\right]_{z=z'-0} = -\frac{1}{2\pi}. \tag{2.4.30}$$

Substituting the two solutions introduced above, and using (2.4.29) we obtain

$$g_s(z|z') = \frac{1}{4\pi\Gamma_s} \exp(-\Gamma_s|z - z'|). \tag{2.4.31}$$

Finally, the explicit expression for the Green's function corresponding to azimuthally symmetric TM modes in a circular waveguide is given by

$$G(r,z|r',z') = \sum_{s=1}^{\infty} \frac{\mathrm{J}_0(p_s r/R)\mathrm{J}_0(p_s r'/R)}{\frac{1}{2}R^2\mathrm{J}_1^2(p_s)} \frac{1}{4\pi\Gamma_s}\exp(-\Gamma_s|z-z'|). \tag{2.4.32}$$

In this expression, we tacitly assumed that $\omega > 0$ and Γ_s is non-zero.

With Green's function established, we can calculate the magnetic vector potential generated by the current distribution described in (2.4.9); the result is

$$\begin{aligned} A_z(r,z,\omega) &= 2\pi\mu_0 \int_0^R \mathrm{d}r' r' \int_{-\infty}^{\infty} \mathrm{d}z' G(r,z|r',z') J_z(r',z') \\ &= -\frac{e\mu_0}{8\pi^2} \sum_{s=1}^{\infty} \frac{\mathrm{J}_0(p_s r/R)}{\frac{1}{2}R^2\mathrm{J}_1^2(p_s)} \frac{2}{\Gamma_s^2 + \omega^2/\mathrm{v}^2} \mathrm{e}^{-j(\omega/\mathrm{v})z}. \end{aligned} \tag{2.4.33}$$

It will be instructive to examine this expression in the *time domain*; the Fourier transform is

$$A_z(r,z,t) = -\frac{e}{2\pi^2\varepsilon_0 R^2} \frac{\beta^2}{1-n^2\beta^2} \sum_{s=1}^{\infty} \frac{\mathrm{J}_0(p_s r/R)}{\mathrm{J}_1^2(p_s)} \int_{-\infty}^{\infty} \mathrm{d}\omega \frac{\mathrm{e}^{j\omega(t-z/\mathrm{v})}}{\omega^2+\Omega_s^2}, \tag{2.4.34}$$

where

$$\Omega_s^2 = \left(\frac{p_s c}{R}\right)^2 \frac{\beta^2}{1-n^2\beta^2}. \tag{2.4.35}$$

Equivalently, this result may be interpreted as the interception of the dispersion relation $-k_z^2 - (p_s/R)^2 + \varepsilon_\mathrm{r}(\omega/c)^2 = 0$ and the "beam-line" $k_z = \omega/\mathrm{v}$. With this definition, the problem has been now simplified to the evaluation of the integral

$$F_s(\tau = t - z/\mathrm{v}) \equiv \int_{-\infty}^{\infty} \mathrm{d}\omega \frac{\mathrm{e}^{j\omega\tau}}{\omega^2+\Omega_s^2}, \tag{2.4.36}$$

which in turn is equivalent to the solution of the following differential equation

$$\left[\frac{\mathrm{d}^2}{\mathrm{d}\tau^2} - \Omega_s^2\right] F_s(\tau) = -2\pi\delta(\tau). \tag{2.4.37}$$

Case I: If the particle's velocity is *slower* than the phase velocity of a plane wave in the medium ($n\beta < 1$) then $\Omega_s^2 > 0$ and the solution for $\tau > 0$ is

$$F_s(\tau > 0) = A_+ \mathrm{e}^{-\Omega_s \tau}, \tag{2.4.38}$$

or

$$F_s(\tau<0) = A_- \mathrm{e}^{\Omega_s \tau}. \tag{2.4.39}$$

As previously, in the case of Green's function, $F_s(\tau)$ has to be continuous at $\tau = 0$ and its derivative is discontinuous:

$$\left(\frac{\mathrm{d}}{\mathrm{d}\tau}F_s(\tau)\right)_{\tau=0^+} - \left(\frac{\mathrm{d}}{\mathrm{d}\tau}F_s(\tau)\right)_{\tau=0^-} = -2\pi. \tag{2.4.40}$$

When the velocity of the particle is smaller than c/n (i.e., $n\beta < 1$) the characteristic frequency Ω_s is real, therefore

$$F_s(\tau) = \frac{\pi}{\Omega_s}\,\mathrm{e}^{-\Omega_s|\tau|}, \tag{2.4.41}$$

and consequently,

$$A_z(r,z,t) = -\frac{e}{2\pi\varepsilon_0 R^2}\,\frac{\beta^2}{1-\beta^2 n^2}\sum_{s=1}^{\infty}\frac{\mathrm{J}_0(p_s r/R)}{\mathrm{J}_1^2(p_s)\Omega_s}\,\mathrm{e}^{-\Omega_s|t-z/\mathrm{v}|}. \tag{2.4.42}$$

This expression represents a *discrete* superposition of evanescent modes attached to the particle.

Case II: If the particle's velocity is *faster* than the phase velocity of a plane wave in the medium $(n\beta > 1)$ then $\Omega_s^2 < 0$. In this case the waves are slower than the particle and there is no electromagnetic field in front of the particle i.e.,

$$F_s(\tau<0) = 0. \tag{2.4.43}$$

By virtue of the continuity at $\tau = 0$ we have for $\tau > 0$

$$F_s(\tau>0) = A_+ \sin(|\Omega_s|\tau). \tag{2.4.44}$$

Substituting these two expressions in (2.4.40) we obtain

$$F_s(\tau) = -\frac{2\pi}{|\Omega_s|}\sin(|\Omega_s|\tau)h(\tau), \tag{2.4.45}$$

and the magnetic vector potential reads

$$A_z(r,z,t) = -\frac{e}{\pi\varepsilon_0 R^2}\,\frac{\beta^2}{n^2\beta^2-1}\sum_{s=1}\frac{\mathrm{J}_0(p_s r/R)}{\mathrm{J}_1^2(p_s)|\Omega_s|}\sin\left[|\Omega_s|\left(t-\frac{z}{\mathrm{v}}\right)\right]h\left(t-\frac{z}{\mathrm{v}}\right), \tag{2.4.46}$$

where $h(\xi)$ is the Heaviside step function. This expression indicates that when the velocity of the particle is larger than c/n, there is a discrete superposition of *propagating* waves traveling behind the particle. Furthermore, all the waves have the same phase velocity which is identical with the velocity of the particle, v. It is important to bear in mind that this result was obtained after tacitly assuming that ε_{r} is frequency independent which generally is not the case, therefore the summation is limited to a finite number of modes. The modes which contribute are determined by the Cerenkov condition $n(\omega = \Omega_s)\beta > 1$.

After we established the magnetic vector potential, let us now calculate the *average power* which trails behind the particle. Firstly, the azimuthal magnetic field is given by

$$\begin{aligned} H_\phi(r,z,t) &= -\frac{1}{\mu_0}\frac{\partial}{\partial r}A_z(r,z,t) \\ &= \frac{1}{\mu_0}\sum_{s=1} A_s \frac{p_s}{R}\mathrm{J}_1\left(p_s\frac{r}{R}\right)\sin\left[|\Omega_s|\left(t-\frac{z}{\mathrm{v}}\right)\right]h\left(t-\frac{z}{\mathrm{v}}\right), \end{aligned} \tag{2.4.47}$$

where

$$A_s = -\frac{e}{\pi\varepsilon_0 R^2}\,\frac{\beta^2}{n^2\beta^2-1}\,\frac{1}{\mathrm{J}_1^2(p_s)|\Omega_s|}. \tag{2.4.48}$$

Secondly, the radial electric field is determined by the electric scalar potential, which in turn is calculated using the Lorentz gauge, and it reads

$$\begin{aligned} E_r(r,z,t) &= -\frac{\partial}{\partial r}\Phi(r,z,t) \\ &= \frac{c^2}{\varepsilon_{\mathrm{r}}\mathrm{v}}\sum_{s=1} A_s \frac{p_s}{R}\mathrm{J}_1\left(p_s\frac{r}{R}\right)\ \sin\left[|\Omega_s|\left(t-\frac{z}{\mathrm{v}}\right)\right]h\left(t-\frac{z}{\mathrm{v}}\right). \end{aligned} \tag{2.4.49}$$

With these expressions, we can calculate the average electromagnetic power trailing the particle. It is given by

$$P = \frac{\mathrm{e}^2\beta c}{2\pi\varepsilon_0\varepsilon_{\mathrm{r}}R^2}\,\frac{1}{\varepsilon_{\mathrm{r}}\beta^2-1}\sum_s \frac{1}{\mathrm{J}_1^2(p_s)}. \tag{2.4.50}$$

Note that for ultra relativistic particle ($\beta \to 1$) the power is independent of the particle's energy. In order to have a measure of the radiation emitted consider a very *small bunch* of $N \sim 10^{11}$ electrons injected in a waveguide whose radius is 9.2 mm. The waveguide is filled with a material whose dielectric coefficient is $\varepsilon_{\mathrm{r}} = 2.6$ and all electrons have the same energy 450 keV. If we were able to keep their velocity constant, then 23 MW of power at 11.4 GHz (first mode, $s = 1$) will trail the bunch.

Further examining this expression we note that the average power is quadratic with the frequency i.e.,

$$P \equiv \sum_{s=1} P_s = \frac{(Ne)^2}{2\pi\varepsilon_0\varepsilon_{\mathrm{r}}\beta c} \sum_{s=1} \frac{|\Omega_s|^2}{[p_s \mathrm{J}_1(p_s)]^2}. \tag{2.4.51}$$

In addition, based on the definition of the Fourier transform of the current density in (2.4.9), we conclude that the current which this macro-particle excites in the s'th mode is $I_s = eN\Omega_s/2\pi$. With this expression, the radiation impedance of the first mode ($s = 1$) is

$$R_{\mathrm{C},1} = \frac{P_1}{\frac{1}{2}|I_1|^2} = \eta_0 \frac{4\pi}{\varepsilon_{\mathrm{r}}\beta[p_1 \mathrm{J}_1(p_1)]^2}. \tag{2.4.52}$$

For a relativistic particle, $\beta \simeq 1$, a dielectric medium $\varepsilon_{\mathrm{r}} = 2.6$ the radiation impedance corresponding to the first mode is $\simeq 1{,}200\,\Omega$ which is one order of magnitude larger than that of a dipole in free space or between two plates. Note that this impedance is independent of the geometry of the waveguide and for an ultra-relativistic particle it is independent of the particle's energy.

2.4.3 Coherent Cerenkov Radiation

Once we established the radiation from a single bunch, it is possible to proceed and investigate a distribution of electrons rather than a point-charge. For an ensemble of electrons the field components are

$$\begin{aligned}
H_\phi &= \frac{1}{\mu_0} \sum_{s=1} A_s \frac{p_s}{R} \mathrm{J}_1\left(p_s \frac{r}{R}\right) \left\langle \mathrm{J}_0\left(p_s \frac{r_i}{R}\right) \sin\left[|\Omega_s|\left(t - \frac{z - z_i}{\mathrm{v}}\right)\right] h\left(t - \frac{z - z_i}{\mathrm{v}}\right) \right\rangle_i \\
E_r &= \frac{c^2}{\varepsilon_{\mathrm{r}}\mathrm{v}} \sum_{s=1} A_s \frac{p_s}{R} \mathrm{J}_1\left(p_s \frac{r}{R}\right) \left\langle \mathrm{J}_0\left(p_s \frac{r_i}{R}\right) \sin\left[|\Omega_s|\left(t - \frac{z - z_i}{\mathrm{v}}\right)\right] h\left(t - \frac{z - z_i}{\mathrm{v}}\right) \right\rangle_i \\
A_s &= -\frac{eN}{\pi\varepsilon_0 R^2} \frac{\beta^2}{n^2\beta^2 - 1} \frac{1}{\mathrm{J}_1^2(p_s)|\Omega_s|}.
\end{aligned} \tag{2.4.53}$$

wherein $\langle \ldots. \rangle$ represents the ensemble average; $N$is the total number of electrons in the bunch. For simplicity sake, we assume that the electrons are uniformly distributed in the radial direction $(0 < r < R_b)$ and the transverse and longitudinal distributions are independent thus

$$H_\phi = \frac{1}{\mu_0}\sum_{s=1} A_s \frac{p_s}{R} \mathrm{J}_1\left(p_s \frac{r}{R}\right)\left\langle \sin\left[|\Omega_s|\left(t - \frac{z - z_i}{\mathrm{v}}\right)\right] h\left(t - \frac{z - z_i}{\mathrm{v}}\right)\right\rangle_i$$

$$E_r = \frac{c^2}{\varepsilon_\mathrm{r}\mathrm{v}}\sum_{s=1} A_s \frac{p_s}{R} \mathrm{J}_1\left(p_s \frac{r}{R}\right)\left\langle \sin\left[|\Omega_s|\left(t - \frac{z - z_i}{\mathrm{v}}\right)\right] h\left(t - \frac{z - z_i}{\mathrm{v}}\right)\right\rangle_i$$

$$A_s = -\frac{eN}{\pi\varepsilon_0 R^2}\frac{\beta^2}{n^2\beta^2 - 1}\frac{1}{\mathrm{J}_1^2(p_s)|\Omega_s|}\frac{2\mathrm{J}_1(p_s R_b/R)}{(p_s R_b/R)}\,. \tag{2.4.54}$$

Defining $\zeta = \mathrm{v}t - z$, the power emitted is given by

$$P(\zeta) = \frac{(eN)^2}{\pi\varepsilon_0\varepsilon_\mathrm{r} R^2}\frac{\mathrm{v}}{n^2\beta^2 - 1}\sum_s \left[\frac{2\mathrm{J}_1(p_s R_b/R)}{(p_s R_b/R)\mathrm{J}_1(p_s)}\right]^2 \left\langle \sin\left[\frac{|\Omega_s|}{\mathrm{v}}(\zeta + z_i)\right] h(\zeta + z_i)\right\rangle_i^2 \tag{2.4.55}$$

In case of a *single bunch* of length Δ, the trailing power is

$$\frac{P_\mathrm{av}}{\frac{(eN)^2\mathrm{v}}{2\pi\varepsilon_0 R^2}} = \frac{1/\varepsilon_\mathrm{r}}{\varepsilon_\mathrm{r}\beta^2 - 1}\sum_s \left[\frac{2\mathrm{J}_1(p_s R_b/R)}{(p_s R_b/R)\mathrm{J}_1(p_s)}\,\mathrm{sinc}\left(\frac{p_s}{2}\frac{\Delta/R}{\sqrt{\varepsilon_\mathrm{r}\beta^2 - 1}}\right)\right]^2 \tag{2.4.56}$$

Figure 2.5 illustrates the normalized spectrum as expressed above as a function of s; note that it decreases rapidly thus the convergence is expected to be quick.

Analysis of the maximum average power trailing behind the bunch reveals that

$$\frac{P_\mathrm{av}}{\frac{(eN)^2\mathrm{v}}{2\pi\varepsilon_0 R^2}} \simeq \frac{\frac{2/\varepsilon_\mathrm{r}}{\varepsilon_\mathrm{r}\beta^2 - 1}}{c_1 + c_2\left(\frac{R_b}{R}\right)^2 + \left(c_3 + c_4\sqrt{\frac{R_b}{R}}\right)\left(\frac{\Delta}{R}\right)^2 \frac{1}{\varepsilon_\mathrm{r}\beta^2 - 1}} \tag{2.4.57}$$

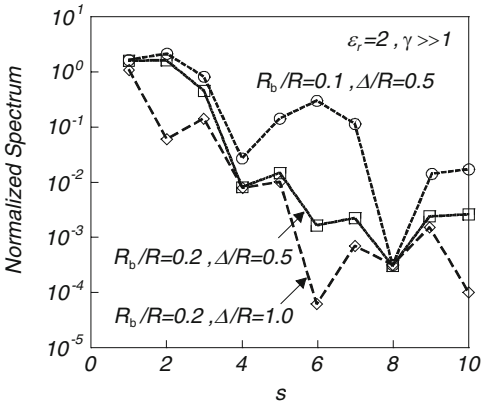

Fig. 2.5 Normalized spectrum of Cerenkov radiation emitted by a finite size azimuthally symmetric bunch in a dielectric filled waveguide of radius R. Only the first 10 modes are shown

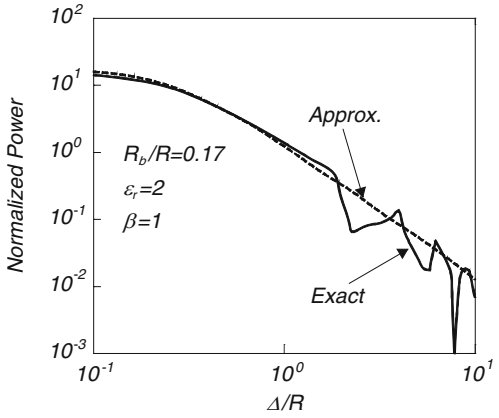

Fig. 2.6 Normalized average power of Cerenkov radiation emitted by a finite size azimuthally symmetric bunch in a dielectric filled waveguide of radius R as a function of the length of the bunch. For the exact expression the first 100 modes have been used. The expression developed reveals an excellent upper value approximation

is an excellent approximation. In this expression $c_1 \simeq 0.0048$, $c_2 \simeq 1.747$, $c_3 \simeq 0.259$ and $c_4 \simeq 1.271$; $0.005 < R_b/R < 0.2$ and $0.1 < \Delta/R < 10$. For a quantitative comparison, Fig. 2.6 shows the exact and the approximate average power generated by a finite size bunch. Some other interesting features are formulated as an Exercise 2.8 at the end of this chapter. In particular, one may investigate ways to *suppress* the coherent radiation.

Taking the same number of electrons (N) but splitting them into a *train of bunches* (M) the discrete spectrum excited in the waveguide undergoes an additional selection associated with the bunches spacing. As in the single bunch case, the bunches are identical in size (radius R_b and length Δ) their spacing is L. A similar approach as above, results into the following expression for the average power trailing behind the train

$$\frac{P_{\rm av}}{\frac{(eN)^2 \mathrm{v}}{2\pi\varepsilon_0 R^2}} = \frac{1/\varepsilon_{\rm r}}{\varepsilon_{\rm r}\beta^2 - 1} \sum_s \left[\frac{2\mathrm{J}_1\left(p_s \frac{R_b}{R}\right)}{p_s \frac{R_b}{R} \mathrm{J}_1(p_s)} \mathrm{sinc}\left(\frac{p_s \Delta/2R}{\sqrt{\varepsilon_{\rm r}\beta^2 - 1}} \right) \frac{\mathrm{sinc}\left(\frac{p_s L/2R}{\sqrt{\varepsilon_{\rm r}\beta^2 - 1}} M \right)}{\mathrm{sinc}\left(\frac{p_s L/2R}{\sqrt{\varepsilon_{\rm r}\beta^2 - 1}} \right)} \right]^2 . \tag{2.4.58}$$

The last term, $\mathrm{sinc}^2(uM)/\mathrm{sinc}^2(u)$, is responsible to the selection associated with the train configuration. If u is not an integer number of π (off resonance condition), then the term is proportional to M^{-2} implying that the total power is reduced by this factor and there is no advantage in splitting the bunch into a train of bunches. However, if we can ensure resonance namely, for a given s the bunch spacing is chosen such that $u \equiv \Omega_s L/2\mathrm{v} = \pi n$, it is possible to generate a total average power that is of the same order of magnitude as if all the electrons were forming a single bunch. In order to reveal this selection associated with the train's configuration it is convenient to normalize the average power to the case of a single bunch $(M = 1)$ – this is illustrated in Fig. 2.7.

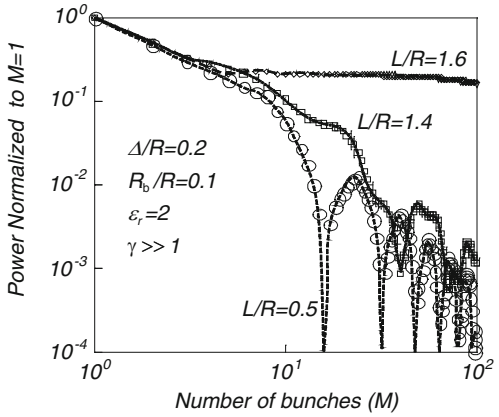

Fig. 2.7 The power normalized to the $M = 1$ case as a function of the number of bunches in the train. Off resonance ($L/R = 0.5, 1.4$), the average power is roughly proportional to M^{-2}. At resonance ($L/R = 1.6$) the power becomes virtually independent of the number of bunches and for large M, this normalized power is of order of unity

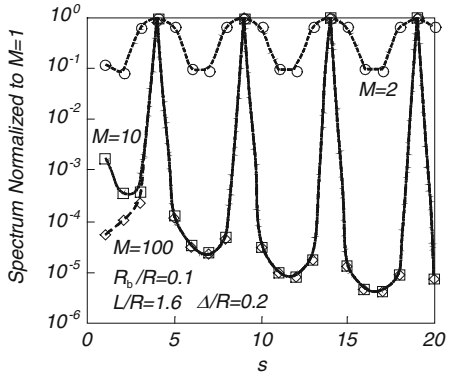

Fig. 2.8 The spectrum normalized to the $M = 1$ case as a funtion of the mode index at resonance ($L/R = 1.6$). At resonant frequencies (corresponding to the frequencies $s = 4, 9, 14.....$) the emitted power is identical to that of the single bunch

When scanning the normalized power there are many possible values of Lthat facilitate power levels of the order of that generated when all the electrons form a single bunch. In the example illustrated in Fig. 2.7, the spacing choice has taken into consideration the fact that for $s \gg 1$, $p_{s+1} - p_s \sim \pi$. This fact facilitates: $u_{s=4} = 3\pi$, $u_{s=9} = 7\pi$, $u_{s=14} = 11\pi$ .... which is reflected in the following plot (Fig. 2.8) of the spectrum of the first 20 modes.

It is evident that at resonance the spectrum is identical to that of a single bunch and in parallel, the spectrum of the off resonance frequencies is significantly suppressed. Note that there is no significant difference between the case $M = 10$ and $M = 100$. For a different choice of bunch-spacing, at resonance, it is possible to have one or at least a few resonant peaks and still to get a substantial fraction of the power generated by a single bunch. The reader is referred to Exercise 2.9 in order to examine additional options associated with the choice of parameters.

2.4.4 Cerenkov Force

In the previous subsection we examined the radiation trailing one or more bunches moving in a dielectric medium with a velocity larger than the phase velocity of a plane wave in the material. Obviously, this emitted energy comes at the expense of its kinetic energy. In other words, the particle is decelerated. It is the goal of this subsection to examine this decelerating force in detail. With this purpose in mind we consider a simple model consisting of a charge $(-e)$ moving at a constant velocity (v) in a vacuum channel of radius R surrounded by a dielectric medium ε_{r}. The evanescent waves attached to the charged particle impinge upon the discontinuity at $r = R$ and they are partially reflected and partially transmitted. It is the *reflected wave* which acts back on the electron decelerating it; the corresponding current density is described by (2.2.15) whereas its time Fourier transform by (2.4.9). Correspondingly, this current density generates a magnetic vector potential determined by

$$A_z(r<R,z,\omega) = 2\pi\mu_0 \int_{-\infty}^{\infty} \mathrm{d}z' \int_0^R \mathrm{d}r' r' G(r,z|r',z') J_z(r',z',\omega) + \int_{-\infty}^{\infty} \mathrm{d}k \rho(k) e^{-jkz} \mathrm{I}_0(\Gamma r), \tag{2.4.59}$$

and

$$A_z(r>R,z,\omega) = \int_{-\infty}^{\infty} \mathrm{d}k \tau(k) \mathrm{e}^{-jkz} \mathrm{K}_0(\Lambda r), \tag{2.4.60}$$

where $\Gamma^2 = k^2 - (\omega/c)^2$, $\Lambda^2 = k^2 - \varepsilon_{\mathrm{r}}(\omega/c)^2$, $G(r',z'|r,z)$ is the boundless Green's function as defined in (2.4.11), (2.4.19) but for vacuum i.e.,

$$G(r',z'|r,z) = \frac{1}{(2\pi)^2} \int_{-\infty}^{\infty} \mathrm{d}k e^{-jk(z-z')} \begin{cases} \mathrm{I}_0(\Gamma r) K_0(\Gamma r') & r<r', \\ K_0(\Gamma r) \mathrm{I}_0(\Gamma r') & r'<r. \end{cases} \tag{2.4.61}$$

The amplitudes ρ and τ represent the reflected and transmitted waves correspondingly. In order to determine these amplitudes we have to impose the boundary conditions at $r = R$. For this purpose, it is convenient to write the solution of the magnetic vector potential off-axis as

$$A_z(0<r<R,z,\omega) = \int_{-\infty}^{\infty} \mathrm{d}k \mathrm{e}^{-jkz} [\rho(k) \mathrm{I}_0(\Gamma r) + \alpha(k) \mathrm{K}_0(\Gamma r)], \tag{2.4.62}$$

where

$$\alpha(k) = -\frac{e\mu_0}{(2\pi)^2} \delta\left(k - \frac{\omega}{\mathrm{v}}\right). \tag{2.4.63}$$

From the continuity of the longitudinal electric field (E_z) we conclude that

$$\frac{c^2}{j\omega}\left[\frac{\omega^2}{c^2}-k^2\right][\rho(k)\mathrm{I}_0(\Gamma R)+\alpha(k)\mathrm{K}_0(\Gamma R)]=\frac{c^2}{j\omega\varepsilon_r}\left[\varepsilon_r\frac{\omega^2}{c^2}-k^2\right]\tau(k)K_0(\Lambda R). \tag{2.4.64}$$

In a similar way the continuity of the azimuthal magnetic field implies

$$\Gamma[\rho(k)\mathrm{I}_1(\Gamma R)-\alpha(k)\mathrm{K}_1(\Gamma R)]=-\Lambda\tau(k)\mathrm{K}_1(\Gamma R). \tag{2.4.65}$$

At this stage, we introduce the (normalized) impedances ratio

$$\zeta\equiv\frac{1}{\varepsilon_\mathrm{r}}\frac{\Lambda}{\Gamma}\frac{\mathrm{K}_0(\Lambda R)}{\mathrm{K}_1(\Lambda R)}, \tag{2.4.66}$$

by whose means the amplitudes of the reflected waves are given by

$$\rho=\alpha\frac{\zeta\mathrm{K}_1(\Gamma R)-\mathrm{K}_0(\Gamma R)}{\zeta\mathrm{I}_1(\Gamma R)+\mathrm{I}_0(\Gamma R)}. \tag{2.4.67}$$

On axis, the only non-zero field is the longitudinal electric field and only the waves "reflected" from the radial discontinuity contribute to the force that acts on the particle, therefore

$$E_z(r=0,z=v_0t,t)=\int_{-\infty}^{\infty}\mathrm{d}\omega dk\frac{c^2}{j\omega}\left[\frac{\omega^2}{c^2}-k^2\right]\rho(\omega,k)\mathrm{e}^{j(\omega-kv)t}. \tag{2.4.68}$$

Substituting the explicit expression for ρ and using the integral over the Dirac delta function [see (2.4.63)] and defining $x=\omega R/c\beta\gamma$, we obtain

$$E_z(r=0,z=v_0t,t)=\frac{-je}{(2\pi)^2\varepsilon_0R^2}\int_{-\infty}^{\infty}\mathrm{d}x x\frac{\zeta(x)\mathrm{K}_1(|x|)-\mathrm{K}_0(|x|)}{\zeta(x)\mathrm{I}_1(|x|)+\mathrm{I}_0(|x|)}. \tag{2.4.69}$$

At this point, it is convenient to define the normalized field that acts on the particle as

$$\begin{aligned}\mathcal{E}&\equiv E_z(r=0,z=\mathrm{v}t,t)\left(\frac{e}{4\pi\varepsilon_0R^2}\right)^{-1}\\&=\frac{2}{\pi}\int_0^{\infty}\mathrm{d}x x\mathrm{Re}\left[\frac{1}{j}\frac{\zeta(x)\mathrm{K}_1(|x|)-\mathrm{K}_0(|x|)}{\zeta(x)\mathrm{I}_1(|x|)+\mathrm{I}_0(|x|)}\right].\end{aligned} \tag{2.4.70}$$

Clearly, from this representation we observe that, for a non-zero force to act on the particle, the impedance ratio ζ has to be complex since the argument of the modified Bessel functions is real.

We can make one step further and simplify this expression by defining

$$\zeta(x) \equiv |\zeta(x)| \mathrm{e}^{j\psi(x)}, \tag{2.4.71}$$

and using $\mathrm{K}_0(x)\mathrm{I}_1(x) + \mathrm{K}_1(x)\mathrm{I}_0(x) = 1/x$, we obtain

$$\mathcal{E} = \frac{2}{\pi} \int_0^\infty \mathrm{d}x \frac{|\zeta(x)| \sin \psi(x)}{\mathrm{I}_0^2(x) + |\zeta(x)|^2 \mathrm{I}_1^2(x) + 2|\zeta(x)| \mathrm{I}_0(x)\mathrm{I}_1(x) \cos \psi(x)}. \tag{2.4.72}$$

In order to evaluate this integral for a dielectric medium and a particle whose velocity βc is larger than $c/\sqrt{\varepsilon_\mathrm{r}}$, we go back to (2.4.66) which now reads

$$\zeta(x) = j \frac{\gamma}{\varepsilon_\mathrm{r}} \sqrt{\varepsilon_\mathrm{r}\beta^2 - 1} \frac{\mathrm{K}_0\left(jx\gamma\sqrt{\varepsilon_\mathrm{r}\beta^2 - 1}\right)}{\mathrm{K}_1\left(jx\gamma\sqrt{\varepsilon_\mathrm{r}\beta^2 - 1}\right)}, \tag{2.4.73}$$

and it can be further simplified if we assume that the main contribution occurs for large arguments of the Bessel function (i.e., $\gamma \gg 1$) thus

$$\zeta(x) \simeq j \frac{\gamma}{\varepsilon_\mathrm{r}} \sqrt{\varepsilon_\mathrm{r}\beta^2 - 1}. \tag{2.4.74}$$

Since subject to this approximation $\psi = \pi/2$ and $|\zeta|$ is constant we can evaluate $\mathcal{E}$,

$$\mathcal{E} = \frac{2}{\pi} \int_0^\infty \mathrm{d}x \frac{|\zeta|}{\mathrm{I}_0^2(x) + |\zeta|^2 \mathrm{I}_1^2(x)}, \tag{2.4.75}$$

for two regimes: firstly when $|\zeta| \gg 1$ i.e., $\gamma \gg 1$, the contribution to the integral is primarily from small values of x thus

$$\mathcal{E} \simeq \frac{2}{\pi} \int_0^\infty \mathrm{d}x \frac{|\zeta|}{1 + |\zeta|^2 x^2/4} \simeq \frac{4}{\pi} \int_0^\infty \mathrm{d}u \frac{1}{1 + u^2} \simeq 2 \tag{2.4.76}$$

At the other extreme ($|\zeta| \ll 1$) the normalized impedance has to be re-calculated and the result is

$$\mathcal{E} \simeq \frac{\gamma^2(\varepsilon_\mathrm{r}\beta^2 - 1)}{\varepsilon_\mathrm{r}} \int_0^\infty \mathrm{d}x \frac{x}{\mathrm{I}_0^2(x)} \simeq 1.263 \frac{\gamma^2(\varepsilon_\mathrm{r}\beta^2 - 1)}{\varepsilon_\mathrm{r}}, \tag{2.4.77}$$

and we can summarize

$$\mathcal{E} \simeq \begin{cases} 0 & \text{for} \quad \beta < 1/\sqrt{\varepsilon_\mathrm{r}}, \\ 1.263\gamma^2\sqrt{\varepsilon_\mathrm{r}\beta^2 - 1}/\varepsilon_\mathrm{r} & \text{for} \quad \gamma \ll \varepsilon_\mathrm{r}/\sqrt{\varepsilon_\mathrm{r}\beta^2 - 1}, \\ 2 & \text{for} \quad \gamma \gg \varepsilon_\mathrm{r}/\sqrt{\varepsilon_\mathrm{r}\beta^2 - 1}. \end{cases} \tag{2.4.78}$$

It is interesting to note that for ultra-relativistic electrons the decelerating Cerenkov force reaches an asymptotic value which is independent of γ and the dielectric coefficient; it is given by $E = -e/2\pi\varepsilon_0 R^2$. In addition, we observe that the normalized impedance (ζ) determines the force.

2.4.5 Ohm Force

If in the Cerenkov case the charged particle has to exceed a certain velocity in order to generate radiation and therefore to experience a decelerating force, in the case of a lossy medium, the moving electron experiences a decelerating force starting from a vanishingly low speed. This is because it excites currents in the surrounding walls and as a result, power is dissipated – which is equivalent to the emitted power in the Cerenkov case. The source of this power is the $\mathbf{J} \cdot \mathbf{E}$ [see (2.1.16)] term which infers the existence of a decelerating force acting on the electron. In order to evaluate this force we use the same formulation as in the previous subsection only that in this case, the dielectric coefficient is complex and it is given by

$$\varepsilon_{\mathrm{r}} = 1 - j\frac{\sigma}{\varepsilon_0 \omega}, \tag{2.4.79}$$

where σ is the (finite) conductivity of the surrounding medium. It is convenient to use the same notation as above, therefore the normalized impedance ζ from (2.4.74) is replaced by

$$\zeta \simeq \frac{1}{1 - j\bar{\sigma}/x}\sqrt{1 + j(\gamma\beta)^2\frac{\bar{\sigma}}{x}}. \tag{2.4.80}$$

In this expression $\bar{\sigma} \equiv \sigma\eta_0 R/\gamma\beta$ which for typical metals and $R \sim 1$ cm is of the order of $10^8/\gamma\beta$ thus for any practical purpose $\bar{\sigma} \gg 1$ hence

$$\zeta \simeq \gamma\beta\sqrt{\frac{x}{\bar{\sigma}}}\exp\left(j\frac{3\pi}{4}\right). \tag{2.4.81}$$

Note that the phase of the normalized impedance is $\psi = 3\pi/4$. Substituting this expression in (2.4.72) and defining the characteristic angular frequency $\omega_0 \equiv 2c/R(\gamma\beta)^3$ as well as the skin-depth $\delta = \sqrt{2/\sigma\mu_0\omega_0}$, we obtain

$$\mathcal{E} = \frac{2}{\pi}\frac{\sqrt{2}}{2}\frac{\delta}{R}\int_0^\infty \mathrm{d}x \frac{\sqrt{x}}{\mathrm{I}_0^2(x) + x\mathrm{I}_1^2(x)\dfrac{\delta^2}{R^2} - \sqrt{2x}\mathrm{I}_0(x)\mathrm{I}_1(x)\dfrac{\delta}{R}} \tag{2.4.82}$$

which can be evaluated analytically for two extreme regimes: in the first case the (normalized) momentum of the particle is much smaller than the normalized

conductivity term i.e., the skin-depth is much smaller than the radius of the tunnel $\delta^2 \ll R^2$ in which case

$$\mathcal{E} \simeq \frac{2}{\pi}\frac{\sqrt{2}}{2}\frac{\delta}{R}\int_0^\infty \mathrm{d}x \frac{\sqrt{x}}{\mathrm{I}_0^2(x)} \simeq 0.54\frac{\delta}{R}. \tag{2.4.83}$$

The second case corresponds to a highly relativistic particle i.e., $(\gamma\beta)^3 \gg \sigma\eta_0 R$ or $\delta^2 \gg R^2$ implying that the main contribution to the integral is from the small values of x which justifies the expansion of the modified Bessel functions in Taylor series. Redefining $y^2 \equiv (x\gamma\beta)^3/4\sigma\eta_0 R$ we have

$$\mathcal{E} \simeq \frac{4\sqrt{2}}{3\pi}\int_0^\infty \mathrm{d}y \frac{1}{1+y^2-y\sqrt{2}} \simeq 2. \tag{2.4.84}$$

In fact a best fit to the exact expression in (2.4.82) reveals that

$$\mathcal{E} \simeq \left(0.54\frac{\delta}{R}+2\frac{\delta^2}{R^2}\right)\left[1+\left(\frac{\delta^2}{R^2}\right)^{\frac{6}{10}}\right]^{-\frac{10}{6}} \tag{2.4.85}$$

is an excellent approximation – the integrated $(0<\delta/R<20)$ relative error is less than 0.02% . Clearly, as in the Cerenkov case, for ultra-relativistic particles $(\gamma^3 \gg \sigma\eta_0 R$ or $\delta \gg R)$ the decelerating force is independent of γ and of the material's characteristics. However, the critical γ for operating in this regime is much higher comparing to the Cerenkov case.

The characteristic angular frequency (ω_0) is low for relativistic electrons and consequently, the skin-depth is much larger than the radius and all the bulk material "participates" in the deceleration process. On the other hand, if the frequency is high, then the skin-depth is small (comparing to the radius) and only a thin layer dissipates power, therefore the loss is proportional to δ.

Finally, imagine an interesting situation whereby the conductivity of the material is negative, this is to say that the medium is active, then the phase in (2.4.81) is $\psi = 5\pi/4$ and the force is *accelerating* which means that energy can be transferred from the medium to the electron. We will further elaborate this topic in Chap. 8 in the context of advanced acceleration concepts.

2.5 Finite Length Effects

In all the effects discussed so far, we assumed an infinite system with no reflected waves. In this section, we consider several systems and phenomena associated with reflected waves. When both forward and backward propagating waves coexist, there is a frequency selection associated with the interference of the two. Another byproduct of reflections is tunneling of the field in a region where the wave is below

cutoff. We also examine the radiation generated by a particle as it traverses a geometric discontinuity in a waveguide. We conclude with the evaluation of a wake field generated by a particle in a cavity.

2.5.1 Impedance Discontinuities

In most cases of interest, the waveguide is not uniform and as a result, more than one wave occurs. In order to illustrate the effect of discontinuities we consider next the following problem: a cylindrical waveguide of radius R but, instead of being uniformly filled with one dielectric material, there are three different dielectrics in three different regions

$$\varepsilon_{\mathrm{r}}(z) = \begin{cases} \varepsilon_1 & \text{for} \quad -\infty < z < 0, \\ \varepsilon_2 & \text{for} \quad 0 \le z \le d, \\ \varepsilon_3 & \text{for} \quad d < z < \infty, \end{cases} \tag{2.5.1}$$

as illustrated in Fig. 2.9.

A wave is launched from $z \to -\infty$ towards the discontinuity at $z = 0$. For simplicity we assume that this wave is composed of a single mode (TM_{01} i.e., $s = 1$). The z component of the magnetic vector in the first region ($-\infty < z < 0$) is given by

$$A_z(r, -\infty < z < 0, \omega) = \left[A_{\mathrm{in}} \mathrm{e}^{-\Gamma_1^{(1)} z} + A_\rho \mathrm{e}^{\Gamma_1^{(1)} z}\right] \mathrm{J}_0\left(p_1 \frac{r}{R}\right), \tag{2.5.2}$$

where A_{in} is the amplitude of the incoming wave and A_ρ is the amplitude of the reflected wave; $\Gamma_1^{(1)} = \sqrt{(p_1/R)^2 - \varepsilon_1(\omega/c)^2}$. Between the two discontinuities at $0 < z < d$ the solution has a similar form

$$A_z(r, 0 \le z \le d, \omega) = \left[A_+ \mathrm{e}^{-\Gamma_1^{(2)} z} + A_- \mathrm{e}^{\Gamma_1^{(2)} z}\right] \mathrm{J}_0\left(p_1 \frac{r}{R}\right), \tag{2.5.3}$$

where $\Gamma_1^{(2)} = \sqrt{(p_1/R)^2 - \varepsilon_2(\omega/c)^2}$ In the third region, there is no reflected wave therefore

$$A_z(r, d < z < \infty, \omega) = A_\tau \mathrm{e}^{-\Gamma_1^{(3)}(z-d)} \mathrm{J}_0\left(p_1 \frac{r}{R}\right), \tag{2.5.4}$$

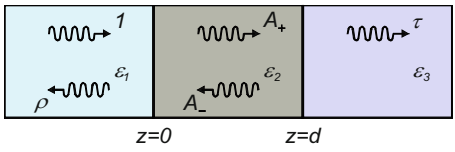

Fig. 2.9 Schematics of the system used to examine the reflected waves resulting from characteristic impedance discontinuities

and as above $\Gamma_1^{(3)} = \sqrt{(p_1/R)^2 - \varepsilon_3(\omega/c)^2}$; A_τ is the amplitude of the transmitted wave. The four as yet unknown amplitudes A_ρ, A_τ, A_+ and A_- are determined by imposing the boundary conditions at $z = 0, d$. Continuity of E_r at $z = 0$ implies

$$Z_1\left(A_{\text{in}} - A_\rho\right) = Z_2(A_+ - A_-); \tag{2.5.5}$$

Z_1 and Z_2 are the characteristic impedances (2.3.26) in the first and second regions respectively. In a similar way the continuity of H_ϕ implies

$$A_{\text{in}} + A_\rho = A_+ + A_-. \tag{2.5.6}$$

An additional set of equations is found imposing the continuity of the same components at $z = d$:

$$Z_2[A_+ \mathrm{e}^{-\psi} - A_- \mathrm{e}^{\psi}] = Z_3 A_\tau, \tag{2.5.7}$$

and

$$A_+ \mathrm{e}^{-\psi} + A_- \mathrm{e}^{\psi} = A_\tau, \tag{2.5.8}$$

where $\psi \equiv \Gamma_1^{(2)} d$. From (2.5.5)–(2.5.8) the reflection (ρ) and transmission (τ) coefficients are determined base on the radial electric field and are given by

$$\begin{aligned} \rho &\equiv \frac{Z_1 A_\rho}{Z_1 A_{\text{in}}} = \frac{\sinh(\psi)(Z_1 Z_3 - Z_2^2) + \cosh(\psi)(Z_1 Z_2 - Z_2 Z_3)}{\sinh(\psi)(Z_1 Z_3 + Z_2^2) + \cosh(\psi)(Z_1 Z_2 + Z_2 Z_3)}, \\ \tau &\equiv \frac{Z_3 A_\tau}{Z_1 A_{\text{in}}} = \frac{Z_3}{Z_1} \frac{2 Z_1 Z_2}{\sinh(\psi)(Z_1 Z_3 + Z_2^2) + \cosh(\psi)(Z_1 Z_2 + Z_2 Z_3)}. \end{aligned} \tag{2.5.9}$$

After we have established the amplitudes of the magnetic vector potential it is possible to determine the electromagnetic field in each one of the regions, thus we can investigate the power flow in the system. Using Poynting's theorem the power conservation implies that

$$\mathrm{Re}(Z_1)\left[|A_{\text{in}}|^2 - |A_\rho|^2\right] = \mathrm{Re}(Z_3)|A_\tau|^2. \tag{2.5.10}$$

This expression relates the power in the first region to that in the third. It does not depend explicitly on the second region; if, for example, in the third region the wave is below cutoff, the characteristic impedance is imaginary and the right-hand side is zero. Consequently, the absolute value of the reflection coefficient is unity, regardless of what happens in the second region. On the other hand, if in regions 1 and 3 the wave is above cutoff, and in region 2 the wave is below cutoff, we still expect power to be transferred. However, the transmission coefficient decays exponentially with $\psi = \Gamma_1^{(2)} d$

$$\tau \sim \frac{4Z_3Z_2}{(Z_1Z_3 + Z_2^2) + Z_2(Z_1 + Z_3)} e^{-\psi}. \tag{2.5.11}$$

In spite of the discontinuities there can be frequencies at which the reflection coefficient (ρ) is zero if we design the structure such that

$$Z_1Z_3 = Z_2^2 \quad \text{and} \quad \psi = j\pi/2, \tag{2.5.12}$$

as one can conclude by examining the numerator of ρ. The expression in (2.5.12) defines the conditions for the so-called *quarter-λ transformer*. Figure 2.10 shows a typical picture of the transmission coefficient. Note that the peaks in the transmission correspond to constructive interference of the two waves in the central section; the valleys correspond to destructive interference of the same waves. Zero reflections also occur when

$$Z_1 = Z_3 \quad \text{and} \quad \psi = j\pi. \tag{2.5.13}$$

If in the first and third region the wave's frequency is *below cutoff* but in the middle region a wave can propagate, then the system will determine a set of discrete frequencies at which the wave can bounce between the two sections. These eigen-frequencies are determined by the geometric parameters and the dielectric coefficients. We can calculate these frequencies from the poles of the transmission or reflection coefficient, namely from the condition that its denominator is zero:

$$\sinh(\psi)(Z_1Z_3 + Z_2^2) + Z_2 \cosh(\psi)(Z_1 + Z_3) = 0. \tag{2.5.14}$$

Equivalently, one can write equations (2.5.5)–(2.5.8) in a matrix form, set the input term to zero ($A_{\text{in}} = 0$) and look for the non-trivial solution by requiring that

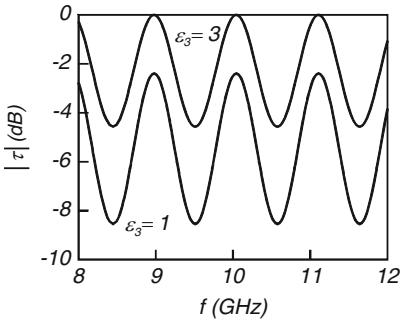

Fig. 2.10 Transmission coefficient as a function of the frequency for two cases: the upper trace represents a situation in which the dielectric coefficient in the third region equals that in the first, therefore at certain frequencies all the power is transferred – see (2.5.13). In the lower trace the two are different and the relation in (2.5.12) is not satisfied, therefore always a fraction of the energy is reflected

the determinant of the matrix is zero – the result is identical with (2.5.14). The reader is encouraged to determine Green's function of the configuration described in this section – see Exercise 2.10.

2.5.2 Geometric Discontinuity

Another source of reflected waves is a *geometric* discontinuity. In a sense these can be conceived as impedance discontinuities but of a more complex character since geometric variations *couple* between the different modes in the waveguide. The simplest configuration which can be considered quasi-analytically consists of a waveguide of radius R_1 and another of radius $R_2 < R_1$; the discontinuity occurs at $z = 0$ as illustrated in Fig. 2.11. A detailed analysis when a single mode impinges upon a discontinuity was reported in the literature e.g., Mittra and Lee (1971) or Lewin (1975).

Step I: We examine first the case when the source term is in the *left-hand side* ($z < 0$), therefore Green's function in the left-hand side has two components

$$G(z<0,r|z'<0,r') = \sum_{s=1}^{\infty} \frac{J_0(p_s r/R_1)J_0(p_s r'/R_1)}{\frac{1}{2}R_1^2 J_1^2(p_s)} \frac{\exp(-\Gamma_s^{(1)}|z-z'|)}{4\pi\Gamma_s^{(1)}} + \sum_{s=1}^{\infty} \rho_s(r',z'<0)\mathrm{J}_0\left(p_s\frac{r}{R_1}\right)\exp\left(\Gamma_s^{(1)}z\right), \tag{2.5.15}$$

the non-homogeneous solution, which corresponds to an infinite waveguide and the homogeneous solution which is due to the discontinuity; $\Gamma_s^{(1)} = \sqrt{(p_s/R_1)^2 - (\omega/c)^2}$. In the right-hand side ($z > 0$),

$$G(z>0,r|z'<0,r') = \sum_{s=1}^{\infty} \tau_s(r',z'<0)\mathrm{J}_0\left(p_s\frac{r}{R_2}\right)\exp\left(-\Gamma_s^{(2)}z\right), \tag{2.5.16}$$

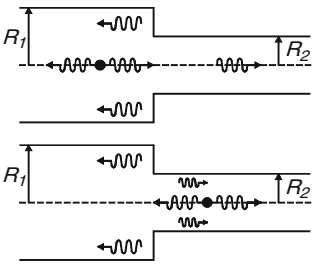

Fig. 2.11 Green's function calculation for one discontinuity in the geometry of a waveguide. In the upper figure the source is in the left and in the lower it is in the right

where $\Gamma_s^{(2)} = \sqrt{(p_s/R_2)^2 - (\omega/c)^2}$. Continuity of the radial electric field at $z = 0$ entails

$$\frac{\partial^2}{\partial z \partial r} G(r, z{=}\,0^- | r', z' < 0) = \begin{cases} \dfrac{\partial^2}{\partial z \partial r} G(r, z{=}\,0^+ | r', z' < 0) & \text{for} \quad 0 \le r < R_2, \\ 0 & \text{for} \quad R_1 \ge r \ge R_2 \end{cases} \tag{2.5.17}$$

In order to determine the amplitudes ρ_s and τ_s the last equation is multiplied by $\mathrm{J}_1(p_s r/R_1)$, the product is integrated from 0 to R_1 and using the orthogonality of the Bessel function [similar to (2.3.17) but for first order Bessel function] we obtain

$$g_s^{(1)}(r', z') - \rho_s(r', z') = \sum_{\sigma=1}^{\infty} Z_{s,\sigma} \tau_\sigma(r', z'), \tag{2.5.18}$$

where

$$g_s^{(1)}(r', z') = \frac{\mathrm{J}_0(p_s r'/R_1)}{\dfrac{1}{2} R_1^2 \mathrm{J}_1^2(p_s)} \frac{\exp\left(\Gamma_s^{(1)} z'\right)}{4\pi \Gamma_s^{(1)}}, \tag{2.5.19}$$

and

$$Z_{s,\sigma} \equiv \frac{\Gamma_\sigma^{(2)}}{\Gamma_s^{(1)}} \frac{p_\sigma}{p_s} \frac{R_1}{R_2} \frac{1}{\mathrm{J}_1^2(p_s)} \frac{2}{R_1^2} \int_0^{R_2} \mathrm{d}r r \mathrm{J}_1\left(p_s \frac{r}{R_1}\right) \mathrm{J}_1\left(p_\sigma \frac{r}{R_2}\right). \tag{2.5.20}$$

Continuity of the azimuthal magnetic field in the domain $0 < r < R_2$ implies

$$\frac{\partial}{\partial r} G(r, z = 0^+ | r', z' < 0) = \frac{\partial}{\partial r} G(r, z = 0^- | r', z' < 0). \tag{2.5.21}$$

As above, we use the fact that in the domain of interest, $\mathrm{J}_1(p_s r/R_2)$ form a complete orthogonal set of functions hence

$$\tau_\sigma(r', z') = \sum_{s=1}^{\infty} Y_{\sigma,s} \left[g_s^{(1)}(r', z') + \rho_s(r', z') \right], \tag{2.5.22}$$

where

$$Y_{\sigma,s} \equiv \frac{2}{{R_1}^2} \int_0^{R_2} \mathrm{d}r r \mathrm{J}_1\left(p_s \frac{r}{R_1}\right) \mathrm{J}_1\left(p_\sigma \frac{r}{R_2}\right). \tag{2.5.23}$$

The integral in both expressions for Z and Y can be calculated analytically (Abramowitz and Stegun 1968, p. 484) and it is given by

$$\int_0^1 \mathrm{d}\xi\xi J_1(p_n\xi)J_1(p_m u\xi) = \begin{cases} \frac{1}{2}\mathrm{J}_1^2(p_n) & \text{for} \quad p_n = p_m u \\ p_m u\left[p_n^2 - p_m^2 u^2\right]^{-1}\mathrm{J}_1(p_n)\mathrm{J}_0(p_m u) & \text{otherwise.} \end{cases} \tag{2.5.24}$$

From (2.5.18), (2.5.22) one can determine the amplitudes of the reflected and transmitted waves. Adopting a vector notation, i.e., $\rho_s(r', z' < 0) \to \mathbf{R}^{(-)}$, $\tau_s(r', z' < 0) \to \mathbf{T}^{(-)}$ and $g_s^{(1)}(r', z' < 0) \to \mathbf{g}^{(1)}$, these amplitudes can be formally written as

$$\mathbf{R}^{(-)} = (I + ZY)^{-1}(I - ZY)\mathbf{g}^{(1)} \tag{2.5.25}$$

and

$$\mathbf{T}^{(-)} = Y\Big[I + (I + ZY)^{-1}(I - ZY)\Big]\mathbf{g}^{(1)}. \tag{2.5.26}$$

Step II: In a similar way, if the source is in the *right-hand side* $(z' > 0)$ then Green's function in the left-hand side can be written as

$$G(z < 0, r|z' > 0, r') = \sum_{s=1}^{\infty} \rho_s(r', z' > 0)\mathrm{J}_0\left(p_s \frac{r}{R_1}\right)\exp\left(\Gamma_s^{(1)} z\right), \tag{2.5.27}$$

and

$$\begin{aligned} G(z > 0, r|z' > 0, r') = &\sum_{s=1}^{\infty} \frac{\mathrm{J}_0(p_s r/R_2)\mathrm{J}_0(p_s r'/R_2)}{\frac{1}{2}R_2^2\mathrm{J}_1^2(p_s)} \frac{\exp\left(-\Gamma_s^{(2)}|z - z'|\right)}{4\pi\Gamma_s^{(2)}} \\ &+ \sum_{s=1}^{\infty} \tau_s(r', z' > 0)\mathrm{J}_0\left(p_s \frac{r}{R_2}\right)\exp\left(-\Gamma_s^{(2)} z\right). \end{aligned} \tag{2.5.28}$$

Continuity of E_r at $z = 0$ implies

$$\rho_s(r', z') = \sum_{\sigma=1}^{\infty} Z_{s,\sigma}\left[g_\sigma^{(2)}(r', z') - \tau_\sigma(r', z')\right], \tag{2.5.29}$$

where

$$g_s^{(2)}(r', z') = \frac{\mathrm{J}_0(p_s r'/R_2)}{\frac{1}{2}R_2^2\mathrm{J}_1^2(p_s)} \frac{\exp\left(-\Gamma_s^{(2)} z'\right)}{4\pi\Gamma_s^{(2)}}, \tag{2.5.30}$$

and the continuity of H_ϕ can be simplified to read

$$\tau_\sigma(r',z') + g_\sigma^{(2)}(r',z') = \sum_{s=1}^{\infty} Y_{\sigma,s}\rho_s(r',z'). \tag{2.5.31}$$

Again, adopting a vector notation $\tau_s(r',z'>0) \to \mathbf{T}^{(+)}$, $g_s^{(2)}(r',z'<0) \to \mathbf{g}^{(2)}$ and $\rho_s(r',z'>0) \to \mathbf{R}^{(+)}$ we can write for the reflected and transmitted waves the following expressions

$$\mathbf{T}^{(+)} = -(I+YZ)^{-1}(I-YZ)\mathbf{g}^{(2)}, \tag{2.5.32}$$

and

$$\mathbf{R}^{(+)} = Z\Big[I + (I+YZ)^{-1}(I-YZ)\Big]\mathbf{g}^{(2)}. \tag{2.5.33}$$

With Green's function established, we calculate now the *energy* emitted by a particle with a charge e as it traverses the discontinuity. Assuming a constant velocity v_0, the current distribution is given by (2.4.9) and the electric field which acts on the particle due to the discontinuity is given by

$$E_z(r,z,\omega) = \frac{e\mathrm{v}_0}{j\omega\varepsilon_0}\left[\frac{\omega^2}{c^2} + \frac{\partial^2}{\partial z^2}\right]\int_{-\infty}^{\infty} \mathrm{d}z' G(r,z|0,z')\exp\left(-j\frac{\omega}{\mathrm{v}_0}z'\right). \tag{2.5.34}$$

With this field component we can examine the total power transferred by the particle i.e.,

$$P(t) = -2\pi\int_{-\infty}^{\infty}\mathrm{d}z\int_0^{R(z)}\mathrm{d}r r J_z(r,z,t)E_z(r,z,t), \tag{2.5.35}$$

and also the total energy defined by

$$W = \int_{-\infty}^{\infty} dt P(t), \tag{2.5.36}$$

which explicitly reads

$$\begin{aligned} W = &-\frac{e^2\mathrm{v}_0}{2\pi\varepsilon_0 R_1^2}\int_{-\infty}^{\infty}\mathrm{d}\omega\frac{1}{j\omega}\sum_{s=1}^{\infty}p_s^2\int_{-\infty}^{0}\mathrm{d}z'\exp\left(-j\frac{\omega}{\mathrm{v}_0}z'\right)\rho_s(0,z') \\ &\times\int_{-\infty}^{0} dt\exp\left[t\left(j\omega+\Gamma_s^{(1)}\mathrm{v}_0\right)\right] \\ &-\frac{e^2\mathrm{v}_0}{2\pi\varepsilon_0 R_2^2}\int_{-\infty}^{\infty}\mathrm{d}\omega\frac{1}{j\omega}\sum_{s=1}^{\infty}p_s^2\int_{0}^{\infty}\mathrm{d}z'\exp\left(-j\frac{\omega}{\mathrm{v}_0}z'\right)\tau_s(0,z') \\ &\times\int_{0}^{\infty} dt\exp\left[t\left(j\omega+\Gamma_s^{(1)}\mathrm{v}_0\right)\right] \end{aligned} \tag{2.5.37}$$

According to (2.5.25), (2.5.32) and the definitions of $g^{(1)}$ and $g^{(2)}$, we can write

$$\rho_s(0, z' < 0) \equiv \sum_{s'} \alpha_{s,s'} \exp\left(\Gamma_{s'}^{(1)} z'\right) \tag{2.5.38}$$

and

$$\tau_s(0, z' > 0) \equiv \sum_{s'} \chi_{s,s'} \exp\left(-\Gamma_{s'}^{(2)} z'\right). \tag{2.5.39}$$

Consequently, the expression for the total energy reads

$$\begin{aligned} W = & \frac{e^2 \mathrm{v}_0^2}{2\pi\varepsilon_0 R_1^2} \int_{-\infty}^{\infty} \mathrm{d}\omega \frac{1}{j\omega} \sum_{s,s'=1}^{\infty} p_s^2 \frac{\alpha_{s,s'}}{j\omega - \mathrm{v}_0 \Gamma_{s'}^{(1)}} \frac{1}{j\omega + \mathrm{v}_0 \Gamma_s^{(1)}} \\ & - \frac{e^2 \mathrm{v}_0^2}{2\pi\varepsilon_0 R_2^2} \int_{-\infty}^{\infty} \mathrm{d}\omega \frac{1}{j\omega} \sum_{s,s'=1}^{\infty} p_s^2 \frac{\chi_{s,s'}}{j\omega + \mathrm{v}_0 \Gamma_{s'}^{(2)}} \frac{1}{j\omega - \mathrm{v}_0 \Gamma_s^{(2)}}. \end{aligned} \tag{2.5.40}$$

The matrices α and χ are frequency dependent, therefore numerical methods have to be invoked in order to have a quantitative answer regarding the energy transfer. Nevertheless, the spectrum can be readily derived from these two expressions. The first term represents the energy emitted when the particle moves in the left-hand side and the second corresponds to the energy emitted when it moves in the right one. It should be pointed out that each one of the terms has two contributions: a fraction of the energy propagates to the left and the remainder to the right. In the next subsection we present a simpler configuration which allows one to trace analytically the way the electromagnetic field develops in time in the case of reflections. We recommend the reader to solve Exercise 2.11 at the end of the chapter in order to assess the emitted spectrum.

Before concluding, one question needs to be addressed. In principle, the number of modes required to represent the field exactly is infinite, but practically only a finite number of terms is taken into consideration because of the need to invert the matrices numerically. The question is what should be the number of Bessel harmonics necessary for the representation of a discontinuity as the one presented above and what is the error associated with the truncation. In order to answer this question, let us consider a simple function

$$f(r) = \begin{cases} 1 & \text{for} \quad 0 \le r < R_2, \\ 0 & \text{for} \quad R_2 < r \le R_1, \end{cases} \tag{2.5.41}$$

as illustrated in Fig. 2.12.

This function can also be represented by a superposition of Bessel functions:

$$f(r) = \sum_{s=1}^{\infty} f_s \mathrm{J}_0\left(p_s \frac{r}{R_1}\right), \tag{2.5.42}$$

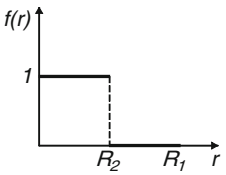

Fig. 2.12 Step function used to model the effect of truncation in a Bessel series representation

where

$$f_s = 2\frac{R_2}{R_1}\frac{\mathrm{J}_1(p_s R_2/R_1)}{p_s \mathrm{J}_1^2(p_s)}; \tag{2.5.43}$$

here we used the fact that the integral

$$\int_0^x \mathrm{d}\xi\xi \mathrm{J}_0(\xi) = x\mathrm{J}_1(x), \tag{2.5.44}$$

can be evaluated analytically (Abramowitz and Stegun 1968, p. 484). We now define the *relative error* made when representing the function only with a finite number of Bessel harmonics as the

$$\mathrm{Error}(N) \equiv \frac{\int_0^{R_1} \mathrm{d}rr\left[f(r) - \sum_{s=1}^{N} f_s \mathrm{J}_0(p_s r/R_1)\right]^2}{\int_0^{R_1} \mathrm{d}rrf^2(r)}. \tag{2.5.45}$$

Using (2.5.43), (2.5.44) the last relation can be simplified to read

$$\mathrm{Error}(N) = 1 - 4\sum_{s=1}^{N}\left[\frac{\mathrm{J}_1(p_s R_2/R_1)}{p_s \mathrm{J}_1(p_s)}\right]^2. \tag{2.5.46}$$

Figure 2.13 illustrates this error. Taking a single mode the normalized error is 36% for $R_2/R_1 = 0.5$ and it drops to 2% for 20 modes. However, even with 20 modes the error can be significantly higher if the radii ratio is small and it is more than 15% for

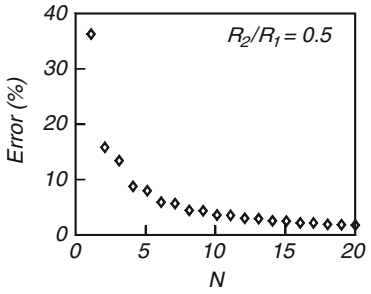

Fig. 2.13 Numerical error as a function of the number of terms

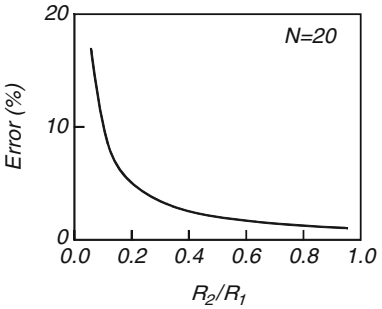

Fig. 2.14 Truncation error as a function of the radius ratio for a constant number of Bessel harmonics

$N = 20$ and $R_2/R_1 \simeq 0.1$ – see Fig. 2.14. These facts become crucial when an accurate solution with multiple discontinuities is necessary.

2.5.3 Wake-Field in a Cavity

In order to examine *transient phenomena* associated with reflected waves we calculate the electromagnetic energy in a cavity as a single point-charge traverses the structure. Consider a *lossless* cylindrical cavity of radius R and length d. A charged particle (e) moves along the axis at a constant velocity v_0. Consequently, the longitudinal component of the current density is the only non-zero term, thus

$$J_z(\mathbf{r},t) = -e\mathrm{v}_0 \frac{1}{2\pi r}\delta(r)\delta(z-\mathrm{v}_0 t). \tag{2.5.47}$$

It excites the longitudinal magnetic vector potential $A_z(\mathbf{r},t)$, which for an azimuthally symmetric system, satisfies

$$\left[\frac{1}{r}\frac{\partial}{\partial r}r\frac{1}{\partial r}+\frac{\partial^2}{\partial z^2}-\frac{1}{c^2}\frac{\partial^2}{\partial t^2}\right]A_z(r,z,t) = -\mu_0 J_z(r,z,t). \tag{2.5.48}$$

In this section, we consider only the internal problem, ignoring the electromagnetic phenomena outside the cavity. The boundary conditions on the internal walls of the cavity impose $E_z(r=R,z,t)=0$, $E_r(r,z=0,t)=0$ and $E_r(r,z=d,t)=0$ therefore, the magnetic vector potential reads

$$A_z(r,z,t) = \sum_{s=1,n=0}^{\infty} A_{s,n}(t)\mathrm{J}_0\left(p_s\frac{r}{R}\right)\cos\left(\frac{\pi n}{d}z\right). \tag{2.5.49}$$

Using the orthogonality of the trigonometric and Bessel functions, we find that the amplitude $A_{s,n}(t)$ satisfies

$$\left[\frac{\mathrm{d}^2}{\mathrm{d}t^2}+\Omega_{s,n}^2\right]A_{s,n}(t)=-\frac{e\mathrm{v}_0}{2\pi\varepsilon_0}\frac{1}{\frac{1}{2}R^2\mathrm{J}_1^2(p_s)}\frac{1}{g_n d}\cos\left(\frac{\pi n}{d}\mathrm{v}_0 t\right)\left[h(t)-h\left(t-\frac{\mathrm{v}_0}{d}\right)\right], \tag{2.5.50}$$

where

$$g_n=\begin{cases}1 & \text{for} \quad n=0,\\ 0.5 & \text{otherwise},\end{cases} \tag{2.5.51}$$

and

$$\Omega_{s,n}=c\sqrt{\left(\frac{p_s}{R}\right)^2+\left(\frac{\pi n}{d}\right)^2}, \tag{2.5.52}$$

are the eigen-frequencies of the cavity. Before the particle enters the cavity ($t<0$), no field exists, therefore

$$A_{s,n}(t<0)=0. \tag{2.5.53}$$

For the time the particle is in the cavity namely, $0<t<d/\mathrm{v}_0$, the solution of (2.5.50) consists of the homogeneous and the excitation term:

$$A_{s,n}\left(0<t<\frac{d}{v_0}\right)=B_1\cos(\Omega_{s,n}t)+B_2\sin(\Omega_{s,n}t)+\alpha_{s,n}\cos(\omega_n t), \tag{2.5.54}$$

where

$$\alpha_{s,n}=-\frac{e\mathrm{v}_0}{2\pi\varepsilon_0}\frac{1}{\frac{1}{2}R^2\mathrm{J}_1^2(p_s)}\frac{1}{g_n d}\frac{1}{\Omega_{s,n}^2-\omega_n^2}, \tag{2.5.55}$$

and

$$\omega_n=\frac{\pi n}{d}\mathrm{v}_0. \tag{2.5.56}$$

Since both the magnetic and the electric field are zero at $t=0$, the function $A_{s,n}(t)$ and its first derivative are zero at $t=0$ hence

$$B_1+\alpha_{s,n}=0, \tag{2.5.57}$$

and

$$B_2=0. \tag{2.5.58}$$

Consequently, the amplitude of the magnetic vector potential $[A_{s,n}(t)]$ reads

$$A_{s,n}(t) = \alpha_{s,n}\left[\cos(\omega_n t) - \cos(\Omega_{s,n} t)\right]. \tag{2.5.59}$$

Beyond $t = d/\mathrm{v}_0$, the particle is out of the structure thus the source term in (2.5.50) is zero and the solution reads

$$A_{s,n}\left(t > \frac{d}{\mathrm{v}_0}\right) = C_1 \cos\left[\Omega_{s,n}\left(t - \frac{d}{\mathrm{v}_0}\right)\right] + C_2 \sin\left[\Omega_{s,n}\left(t - \frac{d}{\mathrm{v}_0}\right)\right]. \tag{2.5.60}$$

As in the previous case, at $t = d/\mathrm{v}_0$ both $A_{s,n}(t > d/\mathrm{v}_0)$ and its derivative, have to be continuous:

$$\alpha_{s,n}\left[(-1)^n - \cos\left(\Omega_{s,n}\frac{d}{\mathrm{v}_0}\right)\right] = C_1, \tag{2.5.61}$$

and

$$\alpha_{s,n}\Omega_{s,n}\sin\left(\Omega_{s,n}\frac{d}{\mathrm{v}_0}\right) = C_2\Omega_{s,n}. \tag{2.5.62}$$

For this time-period, the explicit expression for the magnetic vector potential is

$$\begin{aligned} A_{s,n}\left(t > \frac{d}{\mathrm{v}_0}\right) = {} & \alpha_{s,n}\left[(-1)^n - \cos\left(\Omega_{s,n}\frac{d}{\mathrm{v}_0}\right)\right]\cos\left[\Omega_{s,n}\left(t - \frac{d}{\mathrm{v}_0}\right)\right] \\ & + \alpha_{s,n}\sin\left(\Omega_{s,n}\frac{d}{\mathrm{v}_0}\right)\sin\left[\Omega_{s,n}\left(t - \frac{d}{\mathrm{v}_0}\right)\right], \end{aligned} \tag{2.5.63}$$

The expressions in (2.5.53), (2.5.59), (2.5.63) describe the magnetic vector potential in the cavity at all times. Figure 2.15 illustrates schematically this solution.

During the period the electron spends in the cavity, there are two frequencies which are excited: the eigen-frequency of the cavity $\Omega_{s,n}$ and the "resonances" associated with the motion of the particle, ω_n. The latter set corresponds to the case when the phase velocity, $\mathrm{v}_{\mathrm{ph}} = \omega/k$, equals the velocity L/R. Since the boundary conditions impose $k = \pi n/d$ and the resonance implies

$$\mathrm{v}_0 = \mathrm{v}_{\mathrm{ph}} = c\left(\frac{\omega}{c}\frac{d}{\pi n}\right), \tag{2.5.64}$$

thus we can immediately deduce the resonance frequencies ω_n as given in (2.5.56).

Now that the magnetic vector potential has been determined, we consider the effect of the field generated in the cavity on the moving particle. The relevant component is the longitudinal one

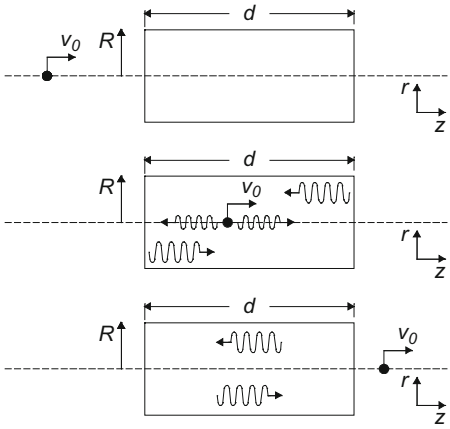

Fig. 2.15 Schematics of the field distribution generated by a particle as it traverse a cavity. Prior to its entrance, no field exists in the cavity. When in the cavity the field has two contributions: directly from the source (non-homogeneous) and reflections from the walls (homogeneous). After the particle leaves the cavity only the homogeneous contribution remains

$$A_z\left(r,z,0<t<\frac{d}{\mathrm{v}_0}\right)=\sum_{s=1,n=0}\alpha_{s,n}\mathrm{J}_0\left(p_s\frac{r}{R}\right)\cos\left(\frac{\pi n}{d}z\right)\left[\cos(\omega_n t)-\cos(\Omega_{s,n}t)\right]. \tag{2.5.65}$$

Note that we omitted the upper limit in the double summation since in practice, the actual dimensions of the particle, which so far was considered infinitesimally small, determines this limit. In order to quantify this statement we realize that the summation is over all eigenmodes which have a wavenumber much longer than the particle's dimension i.e., $\Omega_{s,n}\Delta_z/c<1$ and $p_sR_\mathrm{b}/R<1$wherein Δ_z is the bunch length whereas R_b represents its radius.

According to Maxwell's equations, the longitudinal electric field is

$$\varepsilon_0\frac{\partial}{\partial t}E_z(\mathbf{r},t)=-J_z(\mathbf{r},t)+\frac{1}{r}\frac{\partial}{\partial r}rH_\phi(\mathbf{r},t). \tag{2.5.66}$$

Furthermore, the field that acts on the particle does not include the *self-field*, therefore we omit the current density term. Using the expression for the magnetic vector potential (2.1.32), we have

$$E_z(\mathbf{r},t)=-c^2\int dt\frac{1}{r}\frac{\partial}{\partial r}r\frac{\partial}{\partial r}A_z(\mathbf{r},t), \tag{2.5.67}$$

or explicitly,

$$E_z\left(r,z,0<t<\frac{d}{\mathrm{v}_0}\right)=\sum_{s=1,n=0}\alpha_{s,n}\left(\frac{cp_s}{R}\right)^2\mathrm{J}_0\left(\frac{p_sr}{R}\right)\cos\left(\frac{\pi n}{d}z\right)\left[\frac{\sin(\omega_n t)}{\omega_n}-\frac{\sin(\Omega_{s,n}t)}{\Omega_{s,n}}\right]. \tag{2.5.68}$$

In a lossless and closed cavity the total power flow is zero, therefore Poynting's theorem in its integral form reads

$$\frac{\mathrm{d}W}{\mathrm{d}t} = -2\pi \int_0^R \mathrm{d}r r \int_0^d \mathrm{d}z E_z(r,z,t)\mathrm{J}_z(r,z,t). \tag{2.5.69}$$

Thus substituting the current density (2.5.47) we obtain

$$W = e\mathrm{v}_0 \int_0^{d/\mathrm{v}_0} \mathrm{d}t E_z(r, z = \mathrm{v}_0 t, t), \tag{2.5.70}$$

which has the following explicit form

$$W = e\mathrm{v}_0 \sum_{s=1,n=0} \alpha_{s,n} \left(\frac{cp_s}{R}\right)^2 \int_0^{d/\mathrm{v}_0} \mathrm{d}t \cos(\omega_n t) \left[\frac{\sin(\omega_n t)}{\omega_n} - \frac{\sin(\Omega_{s,n} t)}{\Omega_{s,n}}\right]. \tag{2.5.71}$$

We can evaluate analytically the time integral in this expression. As can be readily deduced, the first term represents the *non-homogeneous* part of the solution and its contribution is identically zero whereas the second's reads

$$W = -e\mathrm{v}_0 \sum_{s=1,n=0} \alpha_{s,n} \left(\frac{cp_s}{R}\right)^2 \frac{1-(-1)^n \cos(\Omega_{s,n} d/\mathrm{v}_0)}{\Omega_{s,n}^2 - \omega_n^2}. \tag{2.5.72}$$

Substituting the explicit expression for $\alpha_{s,n}$ we have

$$\begin{aligned} \bar{W} \equiv W\left(\frac{e^2}{4\pi\varepsilon_0 d}\right)^{-1} &= \sum_{s=1,n=0} \left(\frac{2p_s}{J_1(p_s)}\right)^2 \frac{1}{g_n} \\ &\times \frac{1}{[p_s^2 + (\pi n R/d\gamma)]^2} \left[1 - (-1)^n \cos\left(\frac{\Omega_{s,n}}{\mathrm{v}_0} d\right)\right]. \end{aligned} \tag{2.5.73}$$

Figure 2.16 illustrates the normalized energy excited by a 10 MeV in the first frequencies $\omega < 10\,\Omega_{1,0}$. In this range the spectrum is virtually independent of the particles energy ($\gamma \gg 1$)

$$\bar{W}_{s,n}(\gamma \gg 1) = \left(\frac{2}{J_1(p_s)p_s}\right)^2 \frac{1}{g_n} \left(1 - (-1)^n \cos\frac{\Omega_{s,n}}{c} d\right). \tag{2.5.74}$$

The impact of the homogeneous solution (reflections) on the interaction with electrons will be discussed in detail in Chap. 4 in the context of high power traveling wave tubes. Recently, Sotnikov et al. (2009) recognized that the homogeneous solution (quenching wave) may be of the same order of magnitude as the wake generated in high-gradient dielectric wakefield accelerator.

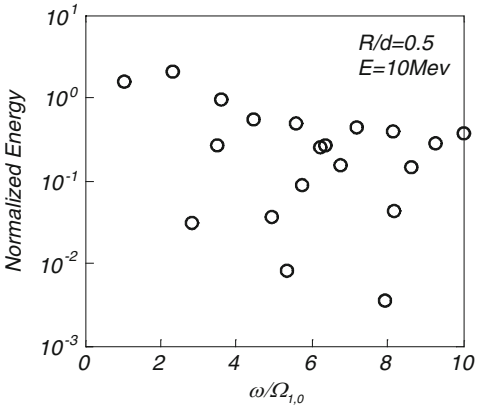

Fig. 2.16 Normalized energy deposited by a 10 MeV point charge in the first modes $(\omega < 10\,\Omega_{1,0})$ of a cylindrical cavity

2.6 Scattered Waves Phenomena

As an electromagnetic wave impinges upon an obstacle, it is scattered. This reflected energy can be harnessed for interaction with charged particles or for measurement purposes. In this section, we consider several cases chosen due to their relative simplicity.

2.6.1 Plane Wave Scattered by a Dielectric Cylinder

As a starting point, let us consider a plane wave that propagates in the x direction and it impinges upon a dielectric (ε_{cyl}) cylinder of radius R whose axis is parallel to the magnetic field component of the incident wave

$$H_z^{(\text{inc})}(x) = H_0 \exp\left(-j\frac{\omega}{c}\sqrt{\varepsilon_{\text{bg}}}x\right); \tag{2.6.1}$$

tacitly assuming a steady state regime $\exp(j\omega t)$ and the background medium is characterized by a dielectric coefficient ε_{bg} – see Fig. 2.17. Based on the generating Bessel function (Abramowitz and Stegun 1968, p. 361)

$$\exp\left[\frac{1}{2}u\left(v-\frac{1}{v}\right)\right] = \sum_{n=-\infty}^{\infty} v^n \mathrm{J}_n(u) \tag{2.6.2}$$

this incident component may be written in cylindrical coordinates $(x = r\cos\phi)$ as

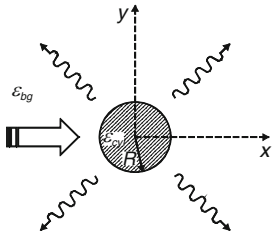

Fig. 2.17 A plane wave scattered by a dielectric cylinder

$$\begin{aligned} H_z^{(\mathrm{inc})}(r,\phi) &= H_0 \exp\Big(-j\frac{\omega}{c}\sqrt{\varepsilon_{\mathrm{bg}}}r\cos\phi\Big) \\ &= H_0 \sum_{n=-\infty}^{\infty} \exp\Big[jn\Big(\phi-\frac{\pi}{2}\Big)\Big]\mathrm{J}_n\Big(\frac{\omega}{c}\sqrt{\varepsilon_{\mathrm{bg}}}r\Big). \end{aligned} \tag{2.6.3}$$

The presence of the cylinder alters the electromagnetic field thus the secondary field is given by

$$H_z^{(\mathrm{sec})}(r,\phi) = H_0 \sum_{n=-\infty}^{\infty} \exp\Big[jn\Big(\phi-\frac{\pi}{2}\Big)\Big] \begin{cases} \tau_n \mathrm{J}_n\Big(\frac{\omega}{c}\sqrt{\varepsilon_{\mathrm{cyl}}}r\Big) & r \le R \\ \rho_n \mathrm{H}_n^{(2)}\Big(\frac{\omega}{c}\sqrt{\varepsilon_{\mathrm{bg}}}r\Big) & r \ge R \end{cases} \tag{2.6.4}$$

For imposing the boundary conditions, it is necessary to specify the azimuthal electric field

$$\begin{aligned} E_\phi^{(\mathrm{inc})}(r,\phi) &= \eta_0 H_0 \sum_{n=-\infty}^{\infty} \exp\Big[jn\Big(\phi-\frac{\pi}{2}\Big)\Big] \frac{j}{\sqrt{\varepsilon_{\mathrm{bg}}}} \dot{\mathrm{J}}_n\Big(\frac{\omega}{c}\sqrt{\varepsilon_{\mathrm{bg}}}r\Big) \\ E_\phi^{(\mathrm{sec})}(r,\phi) &= \eta_0 H_0 \sum_{n=-\infty}^{\infty} \exp\Big[jn\Big(\phi-\frac{\pi}{2}\Big)\Big] \begin{cases} \tau_n \frac{j}{\sqrt{\varepsilon_{\mathrm{cyl}}}} \dot{\mathrm{J}}_n\Big(\frac{\omega}{c}\sqrt{\varepsilon_{\mathrm{cyl}}}r\Big) & r \le R \\ \rho_n \frac{j}{\sqrt{\varepsilon_{\mathrm{bg}}}} \dot{\mathrm{H}}_n^{(2)}\Big(\frac{\omega}{c}\sqrt{\varepsilon_{\mathrm{bg}}}r\Big) & r > R \end{cases} \end{aligned} \tag{2.6.5}$$

Continuity of the two components facilitate to determine the amplitudes

$$\begin{aligned} \rho_n &= \frac{b\dot{\mathrm{J}}_n(b)\dot{\mathrm{J}}_n(a) - a\dot{\mathrm{J}}_n(b)\mathrm{J}_n(a)}{a\dot{\mathrm{J}}_n(b)\mathrm{H}_n^{(2)}(a) - b\mathrm{J}_n(b)\dot{\mathrm{H}}_n^{(2)}(a)}, \\ \tau_n &= b\frac{\dot{\mathrm{J}}_n(a)\mathrm{H}_n^{(2)}(a) - \mathrm{J}_n(a)\dot{\mathrm{H}}_n^{(2)}(a)}{a\dot{\mathrm{J}}_n(b)\mathrm{H}_n^{(2)}(a) - b\mathrm{J}_n(b)\dot{\mathrm{H}}_n^{(2)}(a)} \end{aligned} \tag{2.6.6}$$

where $a = \sqrt{\varepsilon_{\mathrm{bg}}}\omega R/c$ and $b = \sqrt{\varepsilon_{\mathrm{cyl}}}\,\omega R/c$. With the amplitudes established, two measures need to be considered. The first is the extent the cylinder scatters the wave

namely, the *scattering cross-section*. For this purpose we determine the total power scattered in the cylindrical envelope of radius $r \gg R$ and height Δ_z

$$\begin{aligned} P_{\text{scatt}} &= \Delta_z r \int_0^{2\pi} d\phi \text{Re}\left\{\frac{1}{2} E_\phi^{(\text{sec})}(r,\phi)\left[H_z^{(\text{sec})}(r,\phi)\right]^*\right\} \\ &= \Delta_z 2\pi r \left(\frac{\eta_0 |H_0|^2}{2\sqrt{\varepsilon_{\text{bg}}}}\right) \sum_{n=-\infty}^{\infty} |\rho_n|^2 \text{Re}\left\{j\left[\text{H}_n^{(2)}\left(\frac{\omega}{c}\sqrt{\varepsilon_{\text{bg}}} r\right)\right]^* \dot{\text{H}}_n^{(2)}\left(\frac{\omega}{c}\sqrt{\varepsilon_{\text{bg}}} r\right)\right\} \\ &= \Delta_z 2\pi \left(\frac{\eta_0 |H_0|^2}{2\varepsilon_{\text{bg}}}\right) \frac{2}{\pi \frac{\omega}{c}} \sum_{n=-\infty}^{\infty} |\rho_n|^2. \end{aligned} \tag{2.6.7}$$

The scattering cross section is defined by the ratio of the scattered power and the impinging energy flux, $S_x = \frac{1}{2} \frac{\eta_0}{\sqrt{\varepsilon_{\text{bg}}}} |H_0|^2$,

$$\sigma_{\text{scatt}} \equiv \frac{P_{\text{scatt}}}{S_x} = (2R\Delta_z) \frac{2}{a} \sum_{n=-\infty}^{\infty} |\rho_n|^2. \tag{2.6.8}$$

Figure 2.18 illustrates the normalized cross-section ($\bar{\sigma} = \sigma_{\text{scatt}}/2R\Delta_z$) as a function of the frequency.

It reveals the evident resonant character of the cross-section: for a dielectric coefficient $\varepsilon_{\text{cyl}} = 3.3$ and using $N = 100$ azimuthal harmonics, the cross section is almost 4 for $R \simeq 0.4\lambda_0$ and close to unity if the radius is $R \simeq 0.72\lambda_0$. Moreover, if due to dielectric loss, part of the reflected power is absorbed, the effective cross-section is systematically *smaller* than the lossless case.

The opposite is the case if the medium is active, as illustrated in Fig. 2.19. Since multiple reflections in the cylinder may enhance significantly the scattered power, the cross-section may be *larger*. In the figure the range between $0.9 < R/\lambda_0 < 1.2$ has been magnified, and for the specific parameters, the normalized cross section at

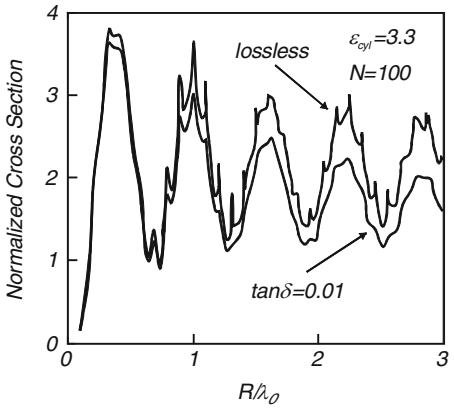

Fig. 2.18 Normalized cross section as a function of the radius normalized to the wavelength in vacuum. Comparing to the lossless case, the cross section in case of a lossy cylinder is systematically smaller since part of the power is absorbed. As a rough estimate $\bar{\sigma}_{\text{lossy}} \sim \bar{\sigma}_{\text{lossless}} \exp[-2\pi(R/\lambda_0)\sqrt{\varepsilon_{\text{cyl}}} \tan\delta]$

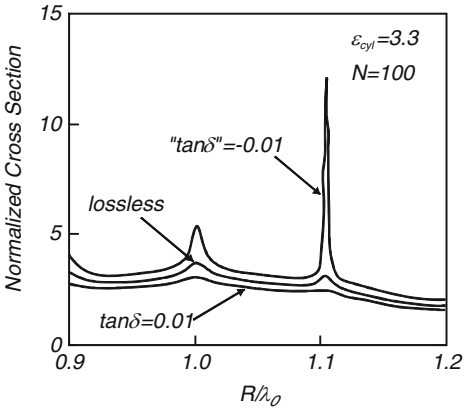

Fig. 2.19 Normalized cross section as a function of the radius normalized to the wavelength in vacuum – focusing in the range $0.9 < R/\lambda_0 < 1.2$. If the medium is active, the cross section can be significantly larger comparing to the lossless case

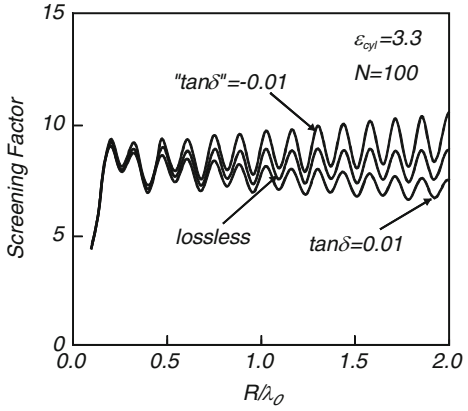

Fig. 2.20 Screening factor as a function of the radius normalized to the wavelength in vacuum. If the medium is active, the cross section can be significantly larger comparing to the lossless case

$R \simeq 1.1\lambda_0$ has dropped from 3.1 to 2.5 due to the dielectric loss but it has increased by almost a factor of four $\bar{\sigma} \sim 12$ in case of an active medium – corresponding to about 11 internal reflections.

The second measure of interest is the *screening factor*, which is indicative of the extent the cylinder reduces/magnifies the electromagnetic energy in its center. This factor may be defined as the ratio of the electromagnetic energy densities at the point of interest with and without the cylinder namely,

$$S \equiv 10\log\left[\frac{w_E^{(\mathrm{tr})}(r=0)+w_M^{(\mathrm{tr})}(r=0)}{w_E^{(\mathrm{inc})}(r=0)+w_M^{(\mathrm{inc})}(r=0)}\right] = 10\log\left(|\tau_0|^2+|\tau_1|^2\right) \qquad (2.6.9)$$

For the parameters mentioned above, the screening factor is illustrated in Fig. 2.20 and evidently, the fiber tends to focus the electromagnetic energy. As may be expected, this focusing is suppressed by lossy material and it is amplified

by active medium. In addition, we observe that lossy or gain medium do not alter the resonant pattern (peaks) associated with azimuthally propagating modes.

2.6.2 Evanescent Waves Scattered by a Dielectric Cylinder

In many cases of interest, waves attached to moving charges are scattered by various obstacles and these radiating modes may be used for the characterization of bunches of electrons as well as of the obstacle. We now exploit the relatively simple configuration of the dielectric cylinder in order to examine the scattering of evanescent waves attached to a charged line (Q/Δ_z) moving with a velocity v at a height $h > R$ – see Fig. 2.21. Near the cylinder the incident field is given by

$$\begin{aligned} H_z^{(\mathrm{inc})}(x, y < h, t) &= -\frac{Q}{4\pi\Delta_z} \int_{-\infty}^{\infty} d\omega \exp\left[j\omega\left(t - \frac{x}{\mathrm{v}}\right) - \frac{|\omega|}{\gamma \mathrm{v}}(h - y)\right] \\ &= -\frac{Q}{4\pi\Delta_z} \int_{-\infty}^{\infty} d\omega \exp(j\omega t) \sum_{n=-\infty}^{\infty} \mathfrak{I}_n(r, \omega, \mathrm{v}) \exp(jn\phi) \\ \mathfrak{I}_n(r, \omega, \mathrm{v}) &\equiv \frac{1}{2\pi} \int_{-\pi}^{\pi} d\phi \exp\left[-jn\phi - j\frac{\omega}{c} r\cos\phi - \frac{|\omega|}{\gamma \mathrm{v}}(h - r\sin\phi)\right] \end{aligned} \tag{2.6.10}$$

Similar to the approach from the above,

$$\begin{aligned} H_z^{(\mathrm{sec})}(r, \phi, t) = &-\frac{Q}{4\pi\Delta_z} \int_{-\infty}^{\infty} d\omega \exp(j\omega t) \\ &\times \sum_{n=-\infty}^{\infty} \exp(jn\phi) \begin{cases} \tau_n(\omega) \mathrm{J}_n\left(\frac{\omega}{c}\sqrt{\varepsilon_{\mathrm{cyl}}} r\right) & r \le R \\ \rho_n(\omega) \mathrm{H}_n^{(2)}\left(\frac{\omega}{c}\sqrt{\varepsilon_{\mathrm{bg}}} r\right) & r \ge R \end{cases} \end{aligned} \tag{2.6.11}$$

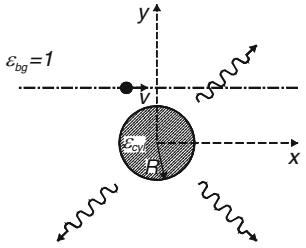

Fig. 2.21 Evanescent waves attached to a moving charged-line are scattered by a cylinder

and

$$
\begin{aligned}
E_{\phi}^{(\mathrm{inc})} &= -\frac{Q}{4\pi\Delta_z}\int_{-\infty}^{\infty} d\omega \exp(j\omega t)\frac{-1}{j\omega\varepsilon_0\varepsilon_{\mathrm{bg}}}\sum_{n=-\infty}^{\infty}\partial_r \mathfrak{I}_n(r,\omega,\mathrm{v})\exp(jn\phi)\\
E_{\phi}^{(\mathrm{sec})} &= -\frac{Q}{4\pi\Delta_z}\int_{-\infty}^{\infty} d\omega \exp(j\omega t)\frac{-1}{j\omega\varepsilon_0}\\
&\quad\times\sum_{n=-\infty}^{\infty}\exp(jn\phi)\begin{cases}\dfrac{1}{\varepsilon_{\mathrm{cyl}}}\tau_n\Big(\dfrac{\omega}{c}\sqrt{\varepsilon_{\mathrm{cyl}}}\Big)\dot{\mathrm{J}}_n\Big(\dfrac{\omega}{c}\sqrt{\varepsilon_{\mathrm{cyl}}}r\Big) & r\le R\\ \dfrac{1}{\varepsilon_{\mathrm{bg}}}\rho_n\Big(\dfrac{\omega}{c}\sqrt{\varepsilon_{\mathrm{bg}}}\Big)\dot{\mathrm{H}}_n^{(2)}\Big(\dfrac{\omega}{c}\sqrt{\varepsilon_{\mathrm{bg}}}r\Big) & r\ge R\end{cases}
\end{aligned}
\tag{2.6.12}
$$

Thus imposing the boundary conditions we obtain the reflection and transmission coefficients

$$
\begin{aligned}
\rho_n &= \frac{b\mathrm{J}_n(b)\dot{\mathfrak{I}}_n - a\dot{\mathrm{J}}_n(b)\mathfrak{I}_n}{a\dot{\mathrm{J}}_n(b)\mathrm{H}_n^{(2)}(a) - b\mathrm{J}_n(b)\dot{\mathrm{H}}_n^{(2)}(a)},\\
\tau_n &= \frac{b\mathrm{H}_n^{(2)}(a)\dot{\mathfrak{I}}_n - b\dot{\mathrm{H}}_n^{(2)}(a)\mathfrak{I}_n}{a\dot{\mathrm{J}}_n(b)\mathrm{H}_n^{(2)}(a) - b\mathrm{J}_n(b)\dot{\mathrm{H}}_n^{(2)}(a)}
\end{aligned}
\tag{2.6.13}
$$

wherein $\dot{\mathfrak{I}}_n(R,\omega,\mathrm{v}) \equiv [R\partial_r\mathfrak{I}_n(r,\omega,\mathrm{v})]_{r=R}/a$, $a=\omega\sqrt{\varepsilon_{\mathrm{bg}}}R/c$, $b=\omega\sqrt{\varepsilon_{\mathrm{cyl}}}R/c$. With the field established, it is possible to determine the emitted energy during the passage of the charged-line near the cylinder

$$
\begin{aligned}
W &= \int_{-\infty}^{\infty} dtP(t) = \Delta_z r\int_{-\pi}^{\pi} d\phi\int_{-\infty}^{\infty} dt\, E_{\phi}^{(\mathrm{sec})}(r,\phi,t)H_z^{(\mathrm{sec})}(r,\phi,t)\\
&= \frac{Q^2}{2\pi\varepsilon_0\Delta_z}\int_{-\infty}^{\infty} da\frac{1}{a}\sum_{n=-\infty}^{\infty}|\rho_n|^2
\end{aligned}
\tag{2.6.14}
$$

which enables us to write the following expression for the normalized spectrum

$$
\frac{d\bar{W}}{da} \equiv \frac{1}{\dfrac{Q^2}{2\pi\varepsilon_0\Delta_z}}\frac{dW}{da} = \frac{2}{a}\sum_{n=-\infty}^{\infty}|\rho_n|^2;
\tag{2.6.15}
$$

it should be pointed out that it has been assumed that the charged-line moves in vacuum thus, $\varepsilon_{\mathrm{bg}}=1$. If the single line charge is replaced by train of M micro-bunches of length $\Delta_{\|}$ and thickness $\Delta_{\perp}$ with a spacing L between each two micro-bunches then the normalized spectrum is

$$\frac{d\bar{W}}{da}=\frac{2}{a}\sum_{n=-\infty}^{\infty}|\rho_n|^2\left[\mathrm{sinc}^2\left(\frac{1}{2}\frac{a}{\beta}\frac{\Delta_\parallel}{R}\right)\frac{\mathrm{sinc}^2\left(\frac{1}{2}M\frac{a}{\beta}\frac{L}{R}\right)}{\mathrm{sinc}^2\left(\frac{1}{2}\frac{a}{\beta}\frac{L}{R}\right)}\mathrm{sinhc}^2\left(\frac{1}{2}\frac{a}{\gamma\beta}\frac{\Delta_\perp}{R}\right)\right]. \tag{2.6.16}$$

Note that the total amount of charge remains Q. For simplicity sake, we assume for what follows that $\varepsilon_{\mathrm{cyl}}\to\infty$ namely, the field does not penetrate in the cylinder therefore $\rho_n=-\dot{\mathfrak{J}}_n/\dot{\mathrm{H}}_n^{(2)}(a)$ and also that the bunch is ultra-relativistic ($\gamma\to\infty$) or if to be more accurate, $\frac{a}{\gamma}\frac{\Delta_\perp}{R},\frac{a}{\gamma}\frac{h}{R}\ll 1$. Since the last two transverse geometric parameters $\frac{\Delta_\perp}{R},\frac{h}{R}$ are expected to be at the most of the order of unity, the previous condition limits the spectrum of our approximation to $a<a_{\mathrm{co}}\equiv 0.01\gamma$. Another implication is a significantly simpler expression for

$$\dot{\mathfrak{J}}_n\equiv\frac{d}{da}\left[\frac{1}{2\pi}\int_{-\pi}^{\pi}d\phi\exp(-jn\phi-ja\cos\phi)\right]=\dot{\mathrm{J}}_n(a)\exp\left(-jn\frac{\pi}{2}\right) \tag{2.6.17}$$

which finally implies

$$\begin{aligned}\frac{d\bar{W}}{da}&=\left[\frac{2}{a}\sum_{n=-\infty}^{\infty}\frac{\dot{\mathrm{J}}_n^2(a)}{\mathrm{J}_n^2(a)+\mathrm{Y}_n^2(a)}\right]\mathrm{sinc}^2\left(\frac{1}{2}\frac{\Delta_\parallel}{R}a\right)\frac{\mathrm{sinc}^2\left(\frac{M}{2}\frac{L}{R}a\right)}{\mathrm{sinc}^2\left(\frac{1}{2}\frac{L}{R}a\right)}\\&\simeq 1.345[1-\exp(-2.5a)]\mathrm{sinc}^2\left(\frac{1}{2}\frac{\Delta_\parallel}{R}a\right)\frac{\mathrm{sinc}^2\left(\frac{M}{2}\frac{L}{R}a\right)}{\mathrm{sinc}^2\left(\frac{1}{2}\frac{L}{R}a\right)}.\end{aligned} \tag{2.6.18}$$

Evidently, the first term represents the contribution of the ideal line-charge whereas the two trailing terms represent the single bunch size effect and the multiple bunches impact respectively.

Before concluding this subsection, two comments are in place. First, the configuration considered above illustrates the coupling between the evanescent waves attached to the moving charged-line and the propagating waves scattered by cylinder. Due to the resemblance to regular diffraction, the emerging waves are also referred to as *diffraction radiation*. Second, we need to provide an alternative interpretation of the emitted spectral density as manifested in (2.6.16). From the way it has been developed, it obviously characterizes the *radiative* contribution far away from the charged-line. Based on Poynting theorem, the source of this radiation is the effect of the secondary field on the charged-line

$$W = \int_{-\infty}^{\infty} dtP(t) = \int_{-\infty}^{\infty} dt\Delta_z \int_{-\infty}^{\infty} dx \int_{-\infty}^{\infty} dyE_x^{(\mathrm{sec})}(x,y,t)J_x(x,y,t)$$
$$= -Q \int_{-\infty}^{\infty} dx \int_{-\infty}^{\infty} d\omega \exp\left(j\frac{\omega}{\mathrm{v}}x\right) E_x^{(\mathrm{sec})}(x,h;\omega) \tag{2.6.19}$$

Using the normalization employed above we get

$$\frac{d\bar{W}}{da} = \bar{Z}_{\|} \equiv -\frac{2\pi}{R\eta_0}\left[\frac{1}{Q/\Delta_z}\int_{-\infty}^{\infty} dx \exp\left(j\frac{\omega}{\mathrm{v}}x\right)E_x^{(\mathrm{sec})}(x,h;\omega)\right] \tag{2.6.20}$$

which clearly reveals that the spectral density of the emitted energy is proportional to the spatial Fourier transform of the electric field *as experienced by the charged-line*. It can be readily checked that the square brackets have units of ohm-meter and consequently, the normalized spectral density equals the, so called, (normalized) *longitudinal impedance* experienced in this case by the charged-line.

2.6.3 Evanescent Waves Scattered by a Metallic Wedge

Diffraction radiation is commonly employed by the particle accelerator community for characterizing the location and to some extent the shape of a charged bunch. This is generally done with thin metallic foils. A model for describing the system, as in the cylinder case, consists of a charged-line (Q/Δ_z) moving at a constant velocity v at a height h above the tip of an ideal wedge $(2\pi - \alpha_2 < \phi < 2\pi - \alpha_1)$ – see Fig. 2.22. In the frequency domain, the magnetic field is a solution of

$$\left[\frac{1}{r}\frac{\partial}{\partial r}r\frac{\partial}{\partial r} + \frac{1}{r^2}\frac{\partial^2}{\partial\phi^2} + \frac{\omega^2}{c^2}\right]H_z(r,\phi,\omega) = \left[\frac{\partial J_x}{\partial y}\right]_{\substack{y=r\sin\phi \\ x=r\cos\phi}} \tag{2.6.21}$$

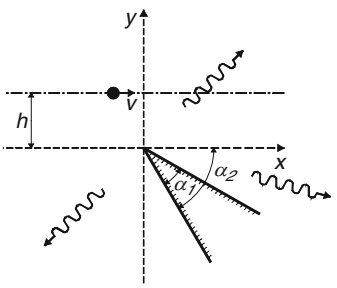

Fig. 2.22 Evanescent waves attached to a moving charged-line are scattered by a wedge

Obviously the radial electric field is zero on both sides of the wedge therefore it is natural to employ the orthogonality of the corresponding azimuthal eigenfunctions namely,

$$H_z(r,\phi,\omega)=\sum_{n=0}^{\infty}H_n(r)\cos[n\pi(\phi+\alpha_1)/(2\pi-\alpha_2+\alpha_1)], \tag{2.6.22}$$

to get

$$\left[\frac{1}{r}\frac{d}{dr}r\frac{d}{dr}-\frac{v^2}{r^2}+\frac{\omega^2}{c^2}\right]H_n(r)=S_n(r)\equiv\frac{1}{g_n}\frac{1}{2\pi-\alpha_2+\alpha_1}\int_{-\alpha_1}^{2\pi-\alpha_2}d\phi\,\frac{\partial J_x}{\partial y}\cos[v(\phi+\alpha_1)] \tag{2.6.23}$$

with $v=n\pi/(2\pi-\alpha_2+\alpha_1)$. The source term may be simplified

$$\begin{aligned}S_n(r)=&\frac{Q}{2\pi\Delta_z}\frac{1}{g_n}\frac{(-v)}{2\pi-\alpha_2+\alpha_1}\frac{1}{r}\int_{-\alpha_1}^{2\pi-\alpha_2}d\phi\exp\left(j\frac{\omega}{\mathrm{v}}r\cos\phi\right)\\&\times\sin[v(\phi+\alpha_1)]\cos\phi\,\delta(y-h)\end{aligned} \tag{2.6.24}$$

Next, we define $\phi_0=\arcsin(h/r)$ and take advantage of the Dirac delta function

$$\delta(y-h)=\frac{u(r-h)}{\sqrt{r^2-h^2}}[\delta(\phi-\phi_0)+\delta(\phi-\pi+\phi_0)] \tag{2.6.25}$$

Wherein $u(x)$ denotes the Heaviside step function thus

$$\begin{aligned}S_n(r)=&\frac{-Q}{2\pi\Delta_z}\frac{v}{g_n}\frac{u(r-h)}{2\pi-\alpha_2+\alpha_1}\frac{1}{r^2}\left\{\exp\left(j\frac{\omega}{\mathrm{v}}\sqrt{r^2-h^2}\right)\sin[v(\phi_0+\alpha_1)]\right.\\&\left.-\exp\left(-j\frac{\omega}{\mathrm{v}}\sqrt{r^2-h^2}\right)\sin[v(\pi-\phi_0+\alpha_1)]\right\}.\end{aligned} \tag{2.6.26}$$

For a solution of (2.6.23) we employ the corresponding Green's function

$$\mathrm{G}_v(r,r')=j\frac{\pi}{2}\begin{cases}\mathrm{J}_v\left(\frac{\omega}{c}r'\right)\mathrm{H}_v^{(2)}\left(\frac{\omega}{c}r\right) & r>r'\\ \mathrm{H}_v^{(2)}\left(\frac{\omega}{c}r'\right)\mathrm{J}_v\left(\frac{\omega}{c}r\right) & r<r'\end{cases} \tag{2.6.27}$$

and can formally determine the magnetic field

$$H_z(r,\phi,t)=\int_0^{\infty}d\omega\sum_{n=0}^{\infty}\cos[v(\phi+\alpha_1)]\,2\mathrm{Re}\left\{\exp(j\omega t)\int_0^{\infty}dr'\,r'\,\mathrm{G}_v(r,r')S_n(r')\right\} \tag{2.6.28}$$

With this field component established we may proceed and evaluate the *radiated energy* at $r \to \infty$

$$W = \Delta_z r \int_{-\infty}^{\infty} dt \int_{-\alpha_1}^{2\pi-\alpha_2} d\phi E_\phi(r,\phi,t) H_z(r,\phi,t)$$
$$= \eta_0 2\pi \left(\frac{\pi}{2}\right)(2\pi - \alpha_2 + \alpha_1)\Delta_z 2 \int_0^{\infty} d\omega \sum_{n=0}^{\infty} g_n \frac{1}{\frac{\omega}{c}} \left| \int_0^{\infty} dr'\, r'\, \mathrm{J}_\nu\left(\frac{\omega}{c} r'\right) S_n(r') \right|^2 \tag{2.6.29}$$

Defining $\Omega = \omega h/c$, $\bar{W} = W[Q^2/2(2\pi - \alpha_2 + \alpha_1)\varepsilon_0 \Delta_z]^{-1}$ and $\xi = r/h$ the normalized spectral density is given by

$$\frac{d\bar{W}}{d\Omega} = \frac{2}{\Omega} \sum_{n=1}^{\infty} \left| \int_1^{\infty} d\xi \frac{\nu \mathrm{J}_\nu(\Omega\xi)}{\xi} \left\{ \begin{array}{l} \exp\left(j\frac{\Omega}{\beta}\sqrt{\xi^2-1}\right) \sin[\nu(\arcsin(1/\xi)+\alpha_1)] \\ -\exp\left(-j\frac{\Omega}{\beta}\sqrt{\xi^2-1}\right) \sin[\nu(\pi-\arcsin(1/\xi)+\alpha_1)] \end{array} \right\} \right|^2 \tag{2.6.30}$$

or finally, after defining $\xi = 1/\sin\psi$ we obtain

$$\frac{d\bar{W}}{d\Omega} = \frac{2}{\Omega} \sum_{n=1}^{\infty} \left| \int_0^{\pi/2} d\psi \, \frac{\nu \mathrm{J}_\nu\left(\frac{\Omega}{\sin\psi}\right)}{\tan\psi} \left\{ \begin{array}{l} \exp\left(j\frac{\Omega}{\beta}\cot\psi\right) \sin[\nu(\psi+\alpha_1)] \\ -\exp\left(-j\frac{\Omega}{\beta}\cot\psi\right) \sin[\nu(\pi-\psi+\alpha_1)] \end{array} \right\} \right|^2 . \tag{2.6.31}$$

Several observations are in place now that we have an explicit expression for the energy's spectral density. First, note that if the velocity is reversed $\mathrm{v} \to -\mathrm{v}$, this is equivalent to taking the complex conjugate of the term in the curled brackets, the spectral density is *invariant*. At the limit of very low frequencies, the spectral density emitted by a relativistic bunch ($\beta \sim 1$) is *inversely proportional to the frequency* as can be concluded from Fig. 2.23 where we plot this quantity as a function of the normalized frequency(Ω). It should be pointed out that the first twenty harmonics were considered and for fast convergence, the integration was performed in the range $\varepsilon < \psi < \pi/2 - \varepsilon$ where $\varepsilon = 0.0005\pi$. As reference, we also present the first two harmonics ($n = 1, 2$).

Examining the same quantity as a function of the normalized momentum of the bunch we conclude that – see Fig. 2.24 – for $\gamma\beta < 1$ the spectral density is proportional to β^4 (for $\Omega = 1$) however, this dependence is strongly dependent on the normalized frequency. For example, for $\Omega = 0.2$ the spectral density is proportional to $\gamma\beta\left[1 + (\gamma\beta/15)^4\right]^{-1/4}$.

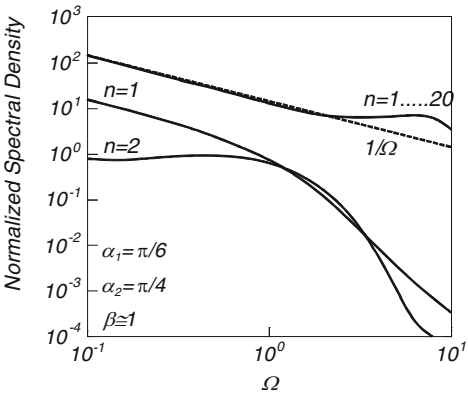

Fig. 2.23 Contribution of the first 20 harmonics to the normalized spectral density as a function of the normalized frequency; $\alpha_1 = \pi/6$, $\alpha_2 = \pi/4$ and $\beta = 1$. The dashed line clearly reveals that this quantity is inversely proportionnal to the frequency for $\Omega < 1$. As reference the first two harmonics are also presented

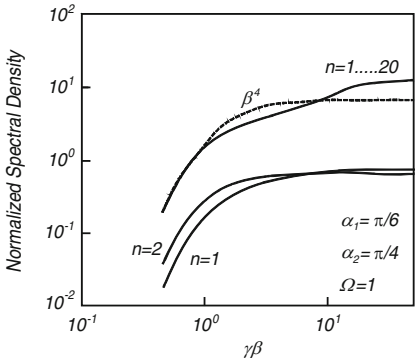

Fig. 2.24 Contribution of the first 20 harmonics to the normalized spectral density as a function of the normalized momentum; $\alpha_1 = \pi/6$, $\alpha_2 = \pi/4$ and $\Omega = 1$. For a relativistic bunch each harmonic reaches it asymptotic value at a different momentum. As reference, the first two harmonics are also plotted. For $\Omega = 1$ the dashed line clearly reveals that the spectral density is proportional to β^4; this dependence may be quite different at other frequencies

Although only the $n = 1$ and $n = 2$ harmonics are illustrated, we found that all harmonics reach an asymptotic value. In fact, this conclusion can be readily deduced from the fact that the energy spectral density depends on β and the latter approaches unity at high kinetic energy. The bending point depends both on the normalized frequency the geometry of the wedge as well as on the harmonic's index.

Exercises

2.1 Determine the boundary condition associated with charge conservation. How it relates to (2.1.12)–(2.1.15)?

2.2 In the context of Sect. 2.2.4, calculate the electromagnetic field associated with the moving charge (2.2.21)–(2.2.22). Calculate the

(continued)

Poynting vector associated with this field. With this result, calculate the total power. Is there a force acting on the moving particle?

2.3 Show that the power radiated in free space by the current distribution in (2.3.2) is given by $P = \eta_0 I^2 (\omega d/c)^2/12\pi$.

2.4 By virtue of the superposition principle, show that in case of multiple "wires" carrying currents I_v located at (x_v, y_v) between the two plates of a radial transmission line the magnetic vector potential is given by

$$A_z = \sum\nolimits_v I_v \frac{1}{4j} H_0^{(2)} \left[\frac{\omega}{c} \sqrt{(x - x_v)^2 + (y - y_v)^2} \right]$$

2.5 Calculate the energy velocity (Sect. 2.3.3) assuming two modes TM_{01} and TM_{02} above cut-off. Plot the energy velocity as a function of the ratio of the two modes $0.3 < \rho = |A_{01}/A_{02}| < 3.0$.

2.6 Calculate the radiation impedance of the TM_{01} in a circular waveguide of radius R. Assume a current distribution

$$J_r(r, z, \omega) = I \Delta_z \mathrm{J}_1(p_1 r/R) \delta(z) p_1/2\pi r R.$$

2.7 The expression that determines the magnetic vector potential of N electrons moving in a dielectric medium ε_r at a velocity v

$$A_z(r, z, \omega) = -\frac{e\mu_0}{(2\pi)^2} \mathrm{K}_0 \left(\frac{\omega}{c} r \sqrt{\frac{c^2}{\mathrm{v}^2} - \varepsilon_\mathrm{r}} \right) \sum_{i=1}^{N} \exp\left[-j \frac{\omega}{\mathrm{v}} (z - z_i) \right]$$

Assuming that the electrons are uniformly distributed $|z_i| \leqslant \Delta/2$, calculate the power emitted by this bunch. Show that the power emitted in the range $\lambda > \Delta$ is proportional to N^2. What happens in the range $\lambda < \Delta$? Repeat the exercise for a Gaussian distribution.

2.8 In Sect. 2.4 we have demonstrated that

$$\frac{P_\mathrm{av}}{\dfrac{(eN)^2 \mathrm{v}}{2\pi\varepsilon_0 R^2}} = \frac{1/\varepsilon_\mathrm{r}}{\varepsilon_\mathrm{r}\beta^2 - 1} \sum_s \left[\frac{2\mathrm{J}_1(p_s R_b/R)}{(p_s R_b/R)\mathrm{J}_1(p_s)} \mathrm{sinc}\left(\frac{p_s}{2} \frac{\Delta/R}{\sqrt{\varepsilon_\mathrm{r}\beta^2 - 1}} \right) \right]^2$$

Determine the condition(s) necessary to suppress the radiation excited in specific mode(s). Can you ensure zero power in many modes? Hint: for large values of s, $p_{s+1} - p_s \sim \pi$.

2.9 Draw the normalized average power (2.4.58) for $M = 100$ normalized to $M = 1$ as a function of L/R as in Fig. 2.7. Show that for specific values of L/R, this quantity is of order of unity. Analyze the spectrum in a few of these cases.

(continued)

2.10 Calculate Green's function associated with the system described in Sect. 2.5.1. Begin with case when the source is located to the left of the discontinuity and continue by solving the problem when the source is between the discontinuities. Can you deduce the Green's function for the third case, when the source is after the third discontinuity, from the first one. For the second case (point-source between the discontinuities) can you design the system such that the source emits zero power?

2.11 Based on (2.5.40), analyze the spectrum of the emitted radiation as a point-charge traverses a geometric discontinuity. Keep the ratio of the number of modes in each region proportional to the radii ratio.

2.12 Based on the formulation of the wake generated by a point charge in a loss-less cavity (Sect. 2.5.3), determine the spectrum of train of N point charges generated in the same cavity. Assume that the spacing between two adjacent charges is L.

2.13 Repeat the steps in Sect. 2.6.1 for the orthogonal polarization, $E_z = E_0 \exp\left(-j\frac{\omega}{c}\sqrt{\varepsilon_{\text{bg}}}x\right)$.

2.14 Analyze the normalized spectrum density in (2.6.16) as a function of the various parameters.

2.15 Plot the contour of constant far-field emitted energy density from a wedge (Sect. 2.6.3) for several values of the kinetic energy; $\alpha_1 = \pi/6$, $\alpha_2 = \pi/4$, $\Omega = 1$ and $\gamma = 2, 11, 21, 31$.

2.16 Extend (2.6.31) to the case of a train of M micro-bunches of spacing L and the length of each one is Δ_x whereas the thickness is Δ_y.

http://www.springer.com/978-3-642-19847-2

Beam-Wave Interaction in Periodic and Quasi-Periodic Structures

Schächter, L.

2011, XVI, 441 p., Hardcover
ISBN: 978-3-642-19847-2